



N73-13824  
MASTER  
COPY:

Report No. M-34  
FIRST GENERATION ATMOSPHERIC PROBES (10-BARS)  
FOR URANUS AND NEPTUNE



IIT RESEARCH INSTITUTE

10 West 35 Street  
Chicago, Illinois 60616

Report No. M-34

FIRST GENERATION ATMOSPHERIC PROBES (10-BARS)  
FOR URANUS AND NEPTUNE

Contributors: R. J. Sullivan  
J. I. Waters  
J. H. Dunkin

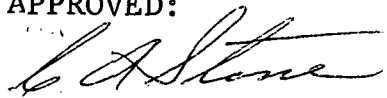
Astro Sciences  
IIT Research Institute  
Chicago, Illinois

for

Planetary Programs Office  
Office of Space Science and Application  
NASA Headquarters  
Washington, D. C.

Contract No. NASW-2144

APPROVED:



C. A. Stone  
Director  
Physics Research

March, 1972

IIT RESEARCH INSTITUTE

## FOREWORD

This is the final report of a study on Uranus-Neptune atmospheric entry probes, performed by IITRI/Astro Sciences for NASA Headquarters (SL). An interim report has previously been issued (Price and Waters 1971); however, considerable revision has taken place since then, and the present report supersedes this interim report.

## SUMMARY

This report presents the results of a preliminary study of first-generation atmospheric entry probe missions to Uranus and Neptune. The probes are envisioned as being deployed from parent spacecraft on two specific Grand Tour missions - a 1979 (launch) Jupiter-Uranus-Neptune mission, and a 1981 Saturn-Uranus-Neptune mission. Shortly before the end of this study, NASA cancelled the Grand Tour program. Nevertheless, it was decided to present the report within the Grand Tour framework. In any case, most of the study results are applicable, at least qualitatively, to other entry probe missions. The probes are designed to survive the high-speed entry, and to descend to an atmospheric depth of 10 bars before data transmission ceases. The final pressure was chosen as a tradeoff between scientific considerations, with respect to which it is extremely important to penetrate at least to this depth, and considerations of probe design, which imply that, if the probe is to penetrate deeper, it must be considerably more massive and complex (because of the required addition of a pressure vessel).

## Trajectories

We have divided the probe trajectory into four phases: approach (trajectory of the parent spacecraft), deployment (period between the probe's release and its first contact with the planet's atmosphere), entry (period of high deceleration), and descent (period of slow penetration through the deep atmosphere). Given the approach trajectory (specified by previous Grand Tour studies),

deflection time, entry point location, and entry time, the other important entry parameters are specified. These include deflection velocity increment, entry velocity, entry angle, spacecraft range and zenith angle at entry, sun zenith angle at entry, and maximum deceleration. Deflection time was chosen as 15 days before entry; this was a tradeoff between larger guidance errors (for earlier times) and higher deflection velocities (for later times). Entry points and entry times were chosen for the four mission cases (i.e. Uranus and Neptune, two Grand Tour trajectories) by a lengthy optimization procedure described in the report. These choices and the corresponding set of entry parameters are given in Table S-1. The two opportunities for Neptune are very similar, because they involve the same periaipse radius of the parent spacecraft (this may be chosen arbitrarily, since Neptune is the last planet on the "tour"). Contrariwise, the Uranus/1981 SUN mission is considerably different from (and inferior to) the Uranus/1979 JUN mission because of the large periaipse radius at Uranus.

Important parameters relating to descent are also listed in Table S-1. Here, the important constraint imposed is the length of time that data can be transmitted between probe and spacecraft after the beginning of entry, which is determined from trajectory dynamics. Not more than  $\sim 30$  minutes may elapse between the beginning of entry and the time the probe reaches its final depth of 10 bars. Descent ballistic coefficients are chosen to fulfill this requirement. The low ballistic coefficient for Neptune requires that the probe descend using a parachute, whereas the higher ballistic coefficient for Uranus eliminates the need for a descent parachute.

TABLE S-1

## ENTRY AND DESCENT PARAMETERS FOR NOMINAL ENTRY POINTS

	Uranus		Neptune	
	1979 JUN	1981 SUN	1979 JUN	1981 SUN
Periapse Radius of Parent Spacecraft	1.63 p.r.	12.77 p.r.	2.0 <sup>a</sup> p.r.	2.0 <sup>a</sup> p.r.
Deflection Time	- 15 days	- 15 days	- 15 days	- 15 days
Deflection Velocity Increment	40 m/s	128 m/s	~ 23 m/s	33 m/s
Entry Point Location <sup>b</sup>	173°, +45°	150°, +12°	-29°, -2°	-43°, -7°
Entry Time	-1.15 hrs	-3.5 hrs	-0.4 hrs	-0.7 hrs
Entry Velocity	27.5 km/s	27.5 km/s	30 km/s	25 km/s
Entry Angle	-50°	-38°	-27°	-41°
S/C Range at Entry	80 K km	345 K km	~ 20 K km	40 K km
S/C Zenith Angle at Entry	23°	3°	10°-20°	~ 20°
Sun Zenith Angle at Entry	42°	72°	67°	50°
Maximum Deceleration	475 g's	550 g's	380 g's	580 g's
Entry Ballistic Coefficient	150 kg/m <sup>2</sup>	150 kg/m <sup>2</sup>	150 kg/m <sup>2</sup>	150 kg/m <sup>2</sup>
Descent Ballistic Coefficient	200 kg/m <sup>2</sup>	200 kg/m <sup>2</sup>	55 kg/m <sup>2</sup>	55 kg/m <sup>2</sup>
Scale Height	21.8 km	21.8 km	12.6 km	12.6 km
Initial Speed of Descent (0.1 bars)	27 km/min	27 km/min	9 km/min	9 km/min
Final Speed of Descent (10 bars)	2 km/min	2 km/min	1 km/min	1 km/min

<sup>a</sup>Periapse at Neptune may be chosen arbitrarily; we chose 2.0 planet radii as an effective compromise between range and line-of-sight motion.

<sup>b</sup>Inertial longitude, latitude.

## Science

Scientific exploration of the atmospheres of Uranus and Neptune would be valuable, not only because these planets are interesting in themselves, but also because understanding of their atmospheric composition would be extremely important for theories of solar system origin. We felt that the most important scientific measurables were (in this order) (1) atmospheric composition, (2) "equation-of-state" variables, i.e. pressure, temperature, and density, and possible presence of condensed phases (clouds), (3) "radiative-transfer" variables, i.e. solar radiation flux and IR radiation emitted from the atmosphere. Using these categories, we chose a scientific payload, which is listed in Table S-2. The mass spectrometer is the primary instrument for measuring composition. However, important ambiguities occur, the most serious involving deuterium compounds. To eliminate this ambiguity, an independent measurement of the hydrogen to deuterium ratio is necessary; this is provided by the H:D photometer. The high and low-g accelerometers together measure the probe's (negative) acceleration throughout entry and descent. The acceleration determines the atmospheric density, and is integrated to provide the probe's speed and altitude as a function of time. Pressure and temperature are also measured. A nephelometer measures cloud density. A visual spectrophotometer measures the solar radiation intensity in several wavelength channels as a function of altitude. Its results may be used to determine the altitude behavior of the optical depth and atmospheric opacity. Finally, the infrared radiometer determines the IR flux emitted from the surrounding atmosphere, for three zenith angles ( $0^\circ$ ,  $90^\circ$  and  $180^\circ$ ) to provide information regarding radiative transfer.



TABLE S-2  
ENTRY PROBE SCIENTIFIC PAYLOAD  
(See Table 8 for references)

Instrument	Mass (kg)	Power (w)	Volume (cm <sup>3</sup> )	Bits per meas.
<u>Composition:</u>				
Mass Spectrometer	4.5	12	5650	345
H-D Photometer	0.5	0.2	100	9
<u>Equation of State:</u>				
High-g accelerometer	0.5	1	100	(28 )
Low-g accelerometer	0.9	2	160	18
Pressure Gauge	0.9	0.1	160	9
Temperature gauge	0.5	0.2	250	12
Nephelometer	2.0	3	1600	9
<u>Radiative Transfer:</u>				
Visual Spectrophotometer	2.3	0.4	500	40
IR Radiometer	0.5	1.5	410	30
<b>TOTAL</b>	<b>12.6</b>	<b>20.4</b>	<b>8930</b>	



### Probe Design

The probe possesses the capability of storing all data received during the mission. During entry, the high-g accelerometer is expected to generate about 7,000 bits. Then, during descent, further data are accumulated, resulting in a total of about 30,000 bits after 30 minutes. The stored data are scanned and transmitted throughout descent at a rate of 50 bits per second. At this rate the entire storage may be transmitted about four times, ensuring reliability of data reception at Earth.

Table S-3 presents a summary of the probe subsystems. The total estimated mass at entry is 128 kg, and the estimated power consumption during descent is 405 watts. Just before entry, the propellant tanks and deflection engine are jettisoned. After entry the parachute opens and the entry heat-shield drops away. Left behind is a "descent aeroshell" of about the same size and shape, containing appropriate windows for scientific instruments. On Uranus the parachute is then jettisoned, and the probe descends (without tumbling) at a speed determined by the probe's ballistic coefficient, in turn determined by the descent aeroshell configuration. On Neptune the parachute must be retained for a proper descent rate to be achieved.

\* \* \*

Our preliminary description of Uranus-Neptune entry probes is quite similar to that of a Jupiter entry probe described by Ames (1971a). It is considerably simpler than several advanced Jupiter entry probes studied by AVCO (1971) and Martin-Marietta (1971), because it is designed for a much shallower depth and because fewer scientific instruments are required for a first-

generation probe into the relatively cloud-free atmospheres of Uranus and Neptune. On the other hand, because of the similarity of atmospheric entry probe concepts for all the large outer planets, it appears that a common probe design would definitely be possible if this were desired. We conclude that 10-bar probes to Uranus and Neptune would be valuable and feasible.

## TABLE OF CONTENTS

	<u>Page</u>
SUMMARY	
1. INTRODUCTION	1
2. TRAJECTORIES	3
2.1 Approach	5
2.2 Deployment and Entry	8
2.3 Descent	25
3. SCIENTIFIC MEASUREMENTS	35
3.1 Current Knowledge of the Atmospheres of Uranus and Neptune	35
3.2 Scientific Instruments	37
3.2.1 Composition Measurements	38
3.2.2 "Equation of State" Measurements	45
3.2.3 "Radiative Transfer" Measurements	51
3.2.4 Summary of Scientific Payload	59
4. PROBE DESIGN	61
4.1 Data Transmission	61
4.2 Description of Subsystems	66
5. COMPARISON OF RESULTS WITH PREVIOUS STUDIES	71
6. CONCLUSIONS	75
REFERENCES	77

## List of Figures

	Page
1. Approach Conditions at Neptune/1979 JUN	6
2. Approach Conditions at Uranus/1979 JUN	7
3. Mass Loss and Acceleration During Atmospheric Entry at Uranus/1979 JUN, 1981 SUN.	10
4. Mass Loss and Acceleration During Atmospheric Entry at Neptune/1979 JUN	11
5. Mass Loss and Acceleration During Atmospheric Entry at Neptune/1981 SUN	12
6. Entry Parameters: Uranus/1979 JUN	14
7. Entry Parameters: Uranus/1981 SUN	15
8. Entry Parameters: Neptune/1979 JUN, 1981 SUN	16
9. Allowed Region of Entry: Uranus/1979 JUN	19
10. Allowed Region of Entry: Uranus/1981 SUN	20
11. Allowed Region of Entry: Neptune/1979 JUN	21
12. Allowed Region of Entry: Neptune/1981 SUN	22
13. Entry Profile: Uranus/1979 JUN, 1981 SUN	26
14. Entry Profile: Neptune/1979 JUN	27
15. Entry Profile: Neptune/1981 SUN	28
16. Equilibrium Vertical Descent at Uranus	30
17. Equilibrium Vertical Descent at Neptune	31
18. Descent Profile at Uranus	32
19. Descent Profile at Neptune	33
20. Probe Acceleration Versus Time During Descent (Schematic)	49
21. Sunlight Collector (Schematic)	54
22. Data Accumulation and Transmission During Descent (Uranus and Neptune)	64

## List of Tables

Page

1.	Parameters of Grand Tour Trajectories	4
2.	Typical Constraints on Entry Parameters	24
3.	Entry and Descent Parameters for Nominal Entry Points	34
4.	Basic Facts About Uranus and Neptune	36
5.	Possible Constituents of the Atmospheres of Uranus and Neptune	40
6.	Optical Depth and Solar Radiation Attenuation Coefficient as Functions of Atmospheric Depth	55
7.	Infrared Radiation in the Atmosphere of Uranus	57
8.	Entry Probe Scientific Payload	60
9.	Data Parameters for Each Instrument	62
10.	Entry Probe Subsystems	67
11.	Probe Sizes and Ballistic Coefficients	70
12.	Comparison of Results of this Study (Uranus-Neptune) with those by AVCO, Ames, and Martin-Marietta (Jupiter)	72
13.	Instruments Not Included in Scientific Payload	73

## 1. INTRODUCTION

The purpose of this report is to investigate the value and feasibility of atmospheric entry probe missions to Uranus and Neptune, and to present preliminary estimates of mission parameters.

Study of the atmospheres of the outer planets is both interesting in itself and important for theories of solar system origin and evolution. Entry probes are generally considered to provide the most valuable means of studying these planetary atmospheres because of the direct in-situ measurements which they can perform. Entry probe missions to Uranus and Neptune would be extremely interesting. However, the atmospheres of these planets are very poorly understood at present. Assuming that this would essentially still be the case at the time of launch of an entry probe mission, we feel that a first-generation probe should be kept relatively small and simple. Its objective should be to provide basic "first-order" data about the atmosphere, which, if desired, could be used to design more ambitious second-generation missions. This report discusses only survivable probes, i.e. those which survive the high-speed entry and continue to transmit data from the deeper atmosphere. As will be discussed subsequently in more detail, scientific considerations make it highly desirable that such a probe descend to an atmospheric depth of at least 10 bars. On the other hand, probe design becomes considerably more difficult if the instruments must withstand pressures greater than 10 bars. Since we wish to keep the probe as simple, light, and reliable as possible, we have chosen 10 bars as its final penetration depth.

Throughout the study, the assumption was made that entry probe missions would be part of Grand Tour flights. Specifically, the Grand Tour missions considered were (1) Jupiter-Uranus-Neptune (JUN) 1979 and (2) Saturn-Uranus-Neptune (SUN) 1981. As the study was being completed, the Grand Tour was cancelled by NASA.

IIT RESEARCH INSTITUTE

Despite this, we decided to present the study results within the Grand Tour framework. However, most of the study results are applicable, with only minor modifications, to Uranus-Neptune entry probes included on any type of outer planet mission.

In this report, trajectory dynamics is discussed first (Section 2) because it imposes some important constraints upon the total time available for data transmission, which in turn determines the descent rate. This last quantity provides important information for the design of the scientific payload, which is discussed in Section 3. Next (Section 4) is presented a discussion of the probe subsystems. In Section 5 of the present report, a comparison is made between our results and the results of some studies of Jupiter atmospheric entry.



## 2. TRAJECTORIES

The parent spacecraft of the entry probe is a flyby which approaches, then recedes from, the planet. In this study the parent spacecraft was assumed to describe a three-planet Grand Tour trajectory. Two specific Grand Tour missions were chosen: a 1979 (launch) Jupiter-Uranus-Neptune mission, and a 1981 Saturn-Uranus-Neptune mission. Basic parameters of the trajectories for these two missions are given in Table 1. The spacecraft arrives at Uranus 5.5 and 6.7 years after launch, and at Neptune 8.5 and 10.4 years after launch, respectively. At Uranus, the periapse radius is fairly low (1.6 planet radii) for the 1979 mission, but quite high (12.8 planet radii) for the 1981 mission. In each case the periapse at Neptune may be adjusted arbitrarily.

The various phases of the trajectory of the entry probe will be distinguished by the following nomenclature:

Approach: Trajectory of the parent spacecraft (and of the probe before it is released from the spacecraft)

Deployment: Trajectory of the probe between the point of release to the point of first contact with the planet's atmosphere

Entry: Trajectory between the point of first contact, through maximum deceleration, to the point where the aeroshell is jettisoned

Descent: Trajectory between the jettisoning of the aeroshell to the point in the deep atmosphere where data cease to be transmitted (this phase may involve a parachute).

TABLE 1: PARAMETERS OF GRAND TOUR TRAJECTORIES

• JUN 1979: Launch 11-1-79 ( $C3 = 120 \text{ km}^2/\text{sec}^2$ )

	Jupiter	Uranus	Neptune
Accumulated Flight Time (yrs)	1.43	5.44	8.51
Relative Approach Velocity ( $\text{km sec}^{-1}$ )	12.93	17.59	19.64
Periapse (planetary radii <sup>*</sup> )	5.63	1.63	arbitrary

• SUN 1981: Launch 12-11-81 ( $C3 = 140 \text{ km}^2/\text{sec}^2$ )

	Saturn	Uranus	Neptune
Accumulated Flight Time (yrs)	3.04	6.68	10.36
Relative Approach Velocity ( $\text{km sec}^{-1}$ )	11.01	13.51	14.55
Periapse (planetary radii <sup>*</sup> )	4.00	12.77	arbitrary

- \*  $r$  (Jupiter) = 71,372 km
- $r$  (Saturn) = 60,401 km
- $r$  (Uranus) = 25,300 km
- $r$  (Neptune) = 23,600 km

## 2.1 Approach

The spacecraft approach trajectory at Neptune (Figure 1) has a modest inclination to the equatorial plane, and the motion has the same sense (posigrade) as the rotation of the planet. This results in a desirable reduction of both the effective aerodynamic velocity of the probe at entry, and the average post-entry rotation rate of the probe-to-spacecraft line of sight.

The approach situation at Uranus (Figure 2) is much more difficult. The polar axis of this planet is nearly parallel to the ecliptic plane, and at the arrival time of these Grand Tour missions lies approximately along the planet-sun line. The plane of the spacecraft trajectory must also lie near the ecliptic plane, since the spacecraft must continue on to Neptune. Therefore the spacecraft approaches the planet over the north pole, its ground track passing southward, approximately along an inertial meridian. The effectiveness of planetary rotation in reducing both the aerodynamic entry velocity of the probe and the rotation rate of the probe-to-spacecraft line of sight is considerably reduced in comparison with the usual (low inclination) approach.

Large planetary flyby distances result in additional communication power losses for an entry probe, while very close flyby distances cause the probe-to-spacecraft line of sight to rotate rapidly from horizon to horizon, limiting communication time and total data transmission. For Uranus, the two chosen missions exemplify these extremes. The 1979 JUN mission is characterized by a close flyby distance at Uranus with the radius at closest approach equal to 1.6 planet radii, whereas the 1981 SUN spacecraft trajectory passes Uranus at a radius of 12.8 planet radii. The flyby radius can be arbitrarily adjusted at Neptune, since it is the last planet intercepted on either mission.

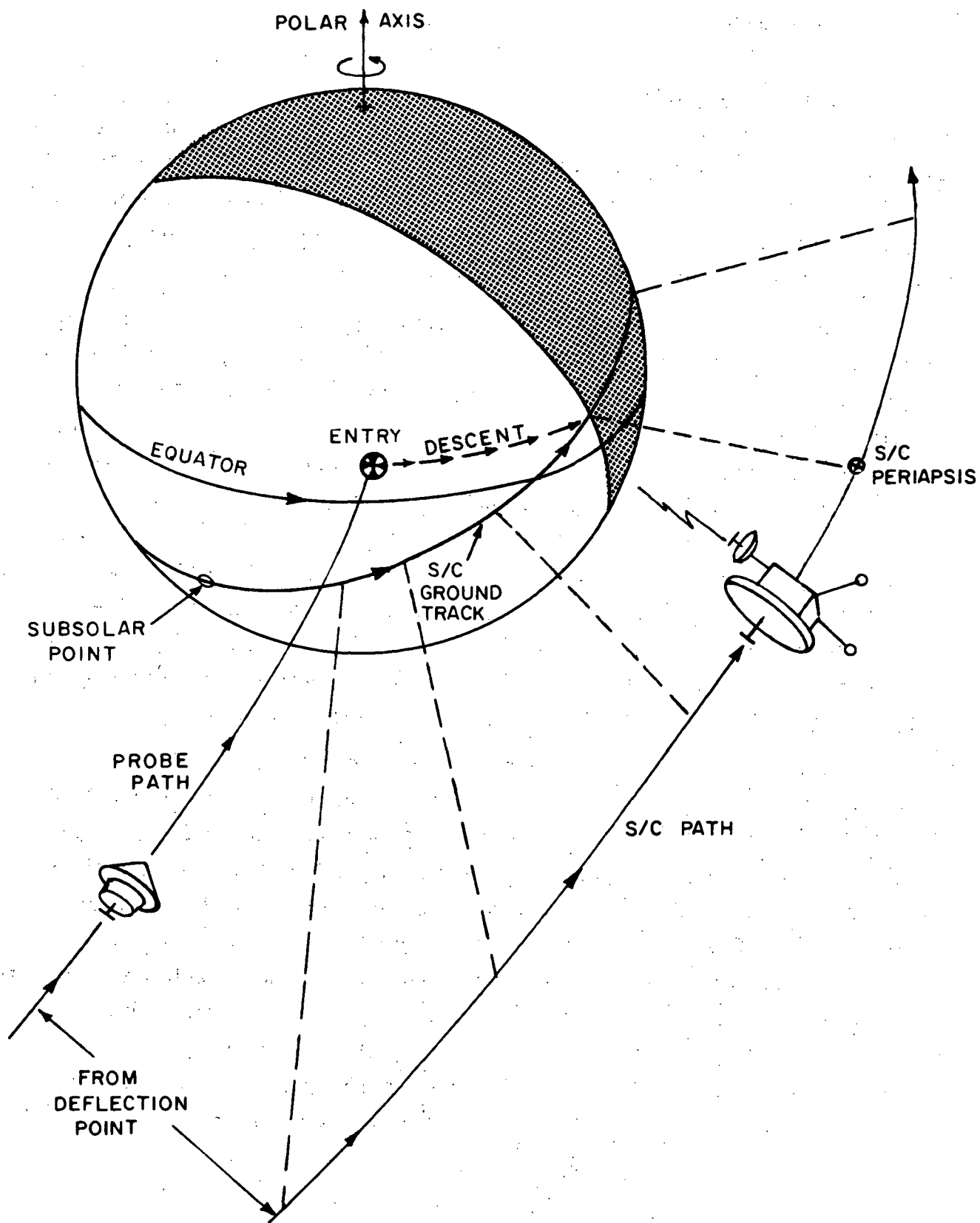


FIGURE 1. APPROACH CONDITIONS AT NEPTUNE / 1979 JUN

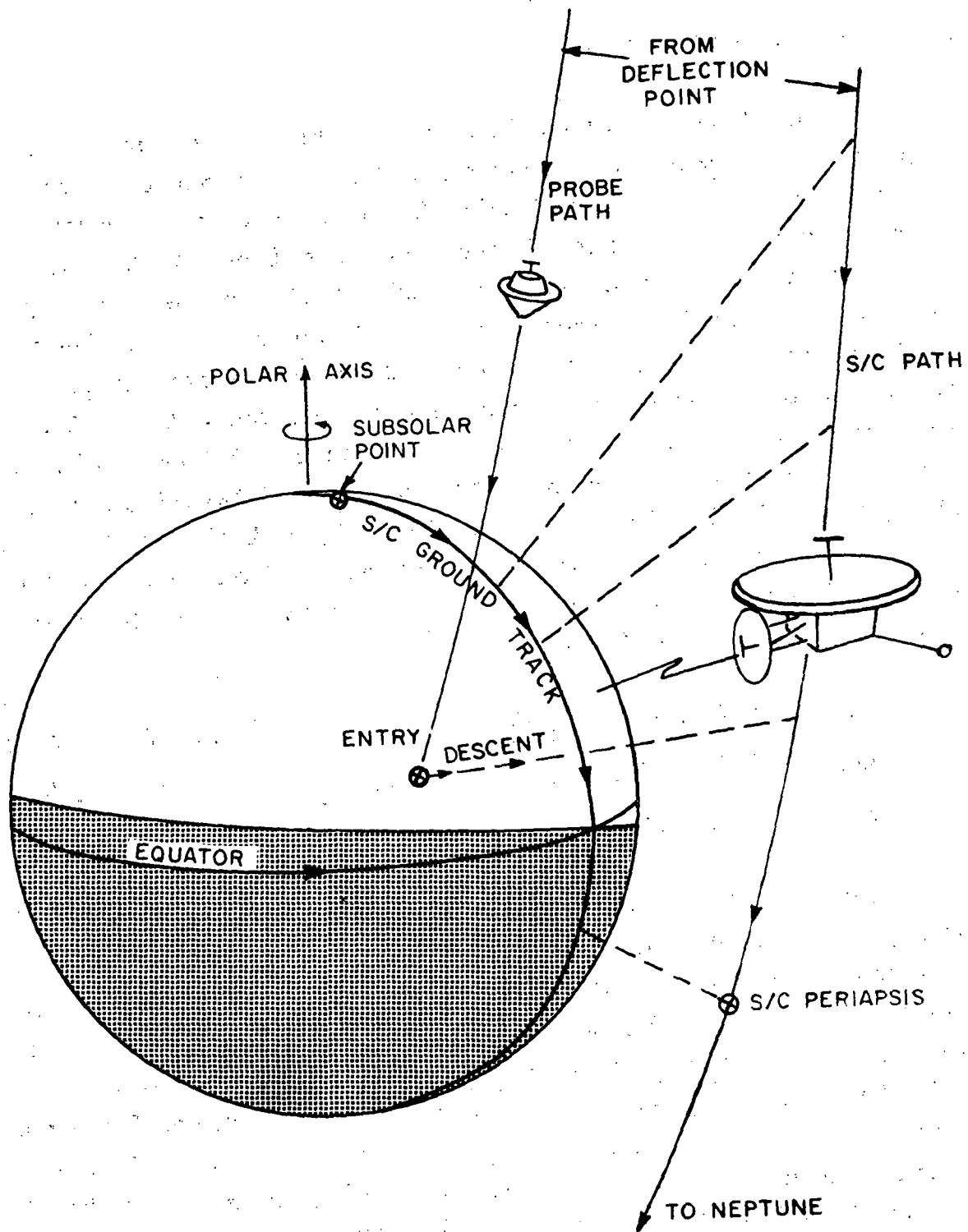


FIGURE 2. APPROACH CONDITIONS AT URANUS / 1979 JUN

## 2.2 Deployment and Entry

Several weeks before the spacecraft reaches periapse, the probe is released and performs a deflection maneuver to alter its trajectory. The time of probe release was chosen to be  $t = -15$  days. (The time of periapse is defined as  $t = 0$ ). This choice was made because, for much earlier values of  $t$  guidance errors are too great, whereas for much later values, deflection velocities are too high. More accurate optimization of deflection time must await a guidance error analysis of the entry point targeting problem, which was beyond the scope of this preliminary study. Given only the approach trajectory and target planet, the probe entry velocity is determined fairly precisely, simply from energy considerations. Significant changes in entry point location alter the entry velocity by only a few percent. For the cases considered, entry velocities are:

Uranus/1979 JUN and 1981 SUN.....	27.5 km/sec
Neptune/1979 JUN.....	30 km/sec
Neptune/1981 SUN.....	25 km/sec.

Peak acceleration at entry acts as an important constraint on entry point location. For this reason it is important to understand the relationship between peak acceleration, mass loss and entry angle. For Jupiter atmospheric entry, between 40 and 50 percent of the entry probe mass must be allocated to the heatshield (including both ablative material and thermal insulation). For Uranus and Neptune, however, the required heatshield mass (including insulation) need not exceed  $\sim 14$  percent\* of the total entry mass (Tauber 1971). This results from the lower entry velocities and less dense atmospheres associated with these

---

\* The ratio of mass ablated to total probe mass is less than  $\sim 8\%$  (Tauber 1971 and Figures 3-5).

planets in comparison with those of Jupiter. We assumed scale heights of 21.8 km and 12.6 km for Uranus and Neptune respectively, which were calculated on the basis of a pure hydrogen atmosphere (Sec. 3.1). On the other hand, since a partial concentration of helium causes greater heating, we decided to be conservative and, for the mass loss coefficients only, assume that the atmospheres were 15% He, 85% H<sub>2</sub> (by numbers). (Strictly speaking, the assumptions regarding scale heights and mass loss coefficients are inconsistent. However, this is negligible compared to the uncertainty surrounding the whole model of an isothermal atmosphere of a given uniform composition. Therefore this inconsistency should cause no concern).

Using these parameters, it was possible to compute approximate mass losses due to ablation of the heatshield during atmospheric entry. The mass loss computations were performed at the NASA Ames Research Center (Tauber 1970), and the results are presented in Figures 3 to 5. These figures show the ablation mass loss and the aerodynamic acceleration plotted against percent of dissipated kinetic energy. The ablation mass loss calculations were made for a ballistic coefficient of 150 kg/m<sup>2</sup>, for which the baseline probe was designed (Sec. 4). The assumed probe diameter was 0.9 meters, about equal to our final baseline choice (Section 4). Also assumed was a cone with a sharp vertex. Therefore, the heating rates near the cone vertex are substantially higher than for a blunted cone (assumed in this study; Sec. 4). However, the effect on overall mass loss is not large because only a small fraction of the body's surface area is subjected to the high heating. For the 60° half-angle forebody geometry considered, convection is the only source of heating for almost all cases (radiation is negligible). Turbulent convection is the major source of mass removal. Substantial uncertainty exists in the treatment of the turbulent boundary layer, especially with large mass ablation, and this fact should be kept in mind when using these results. The approximate doubling of the



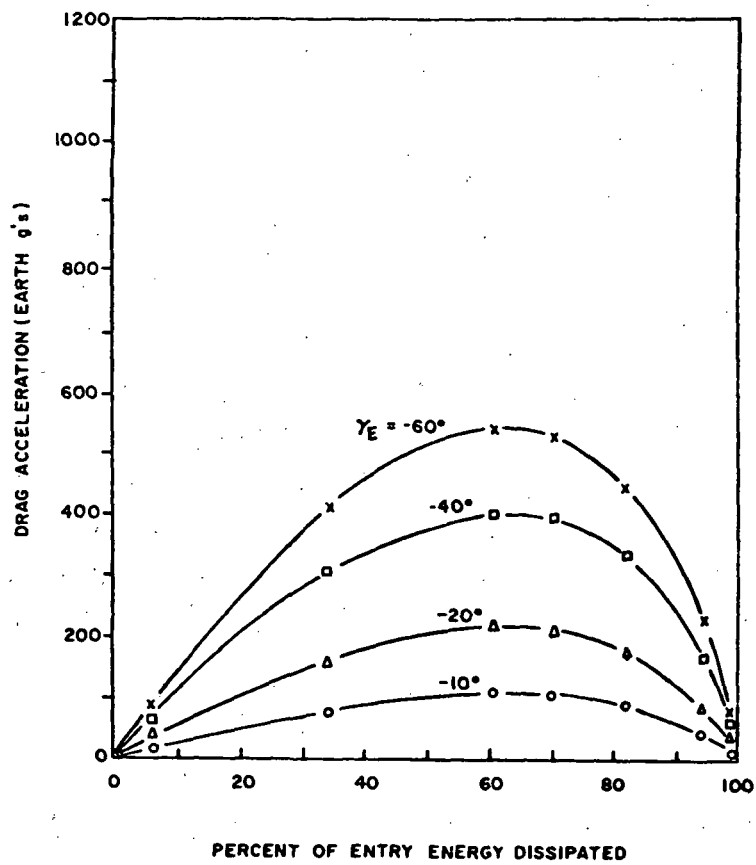
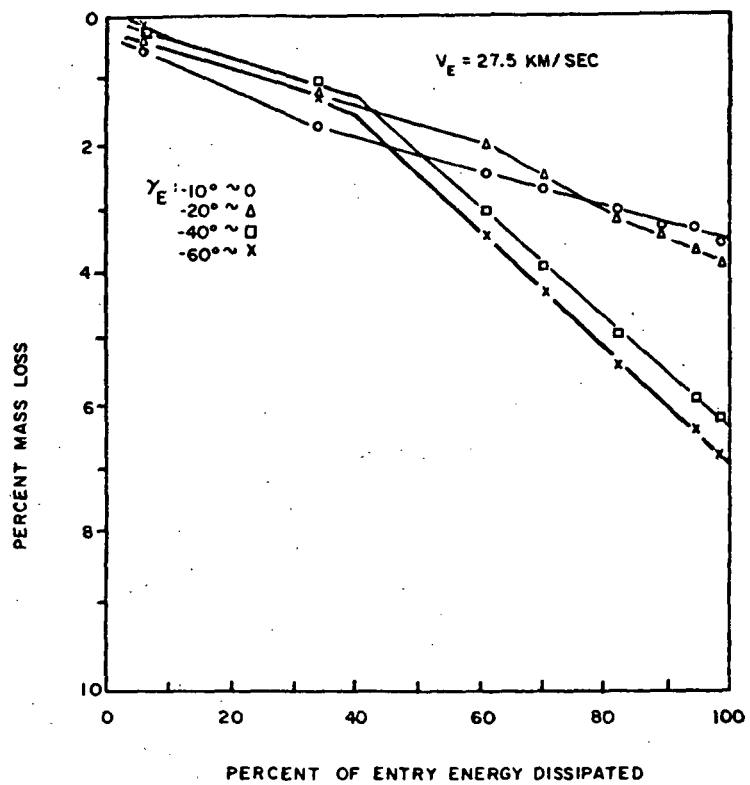


FIGURE 3, MASS LOSS AND ACCELERATION DURING ATMOSPHERIC ENTRY AT URANUS (1979GT, 1981GT)

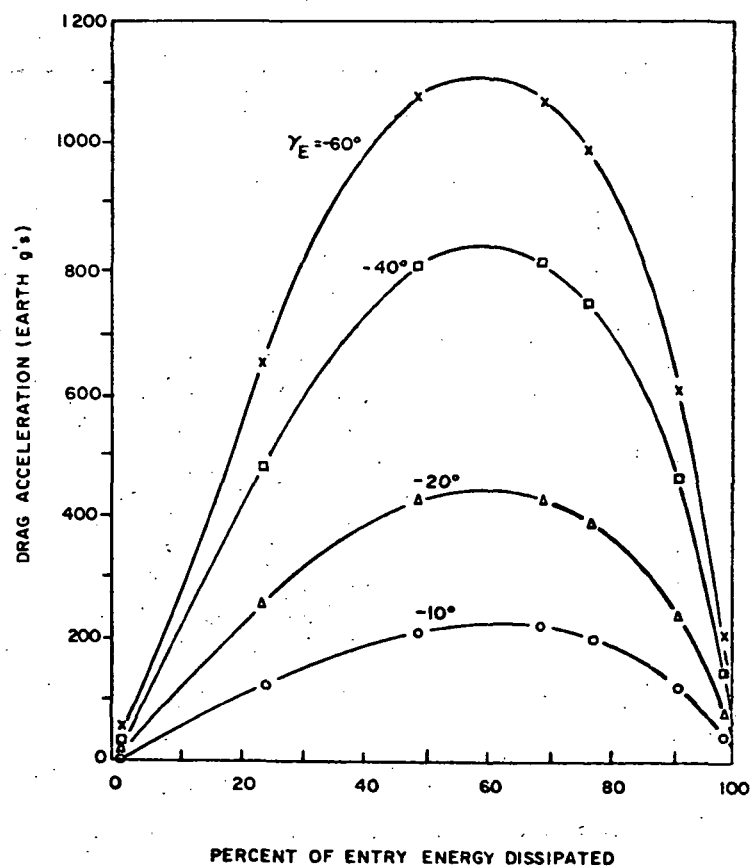
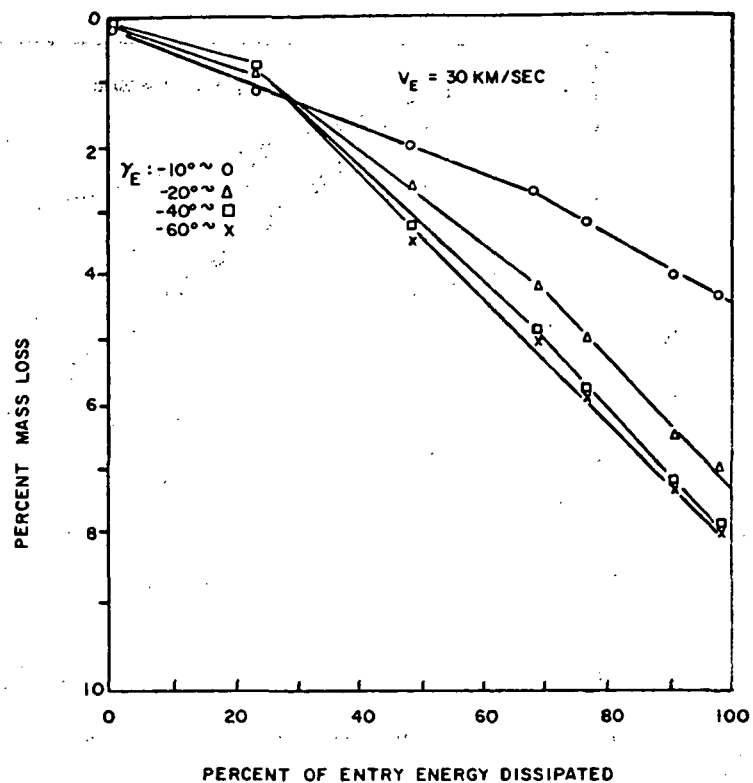


FIGURE 4. MASS LOSS AND ACCELERATION DURING ATMOSPHERIC ENTRY AT NEPTUNE (1979 GT)

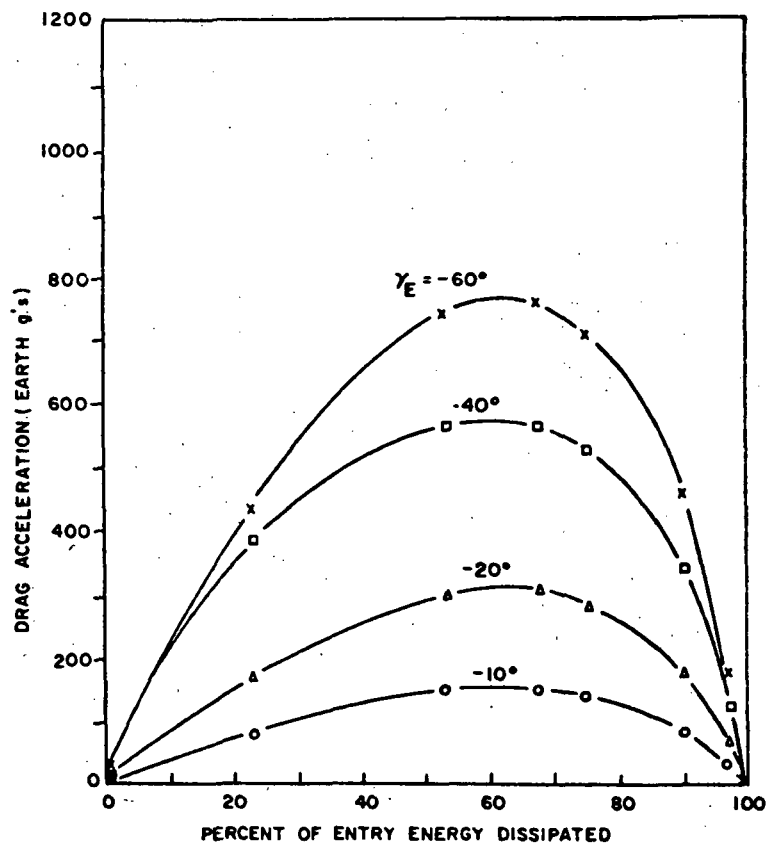
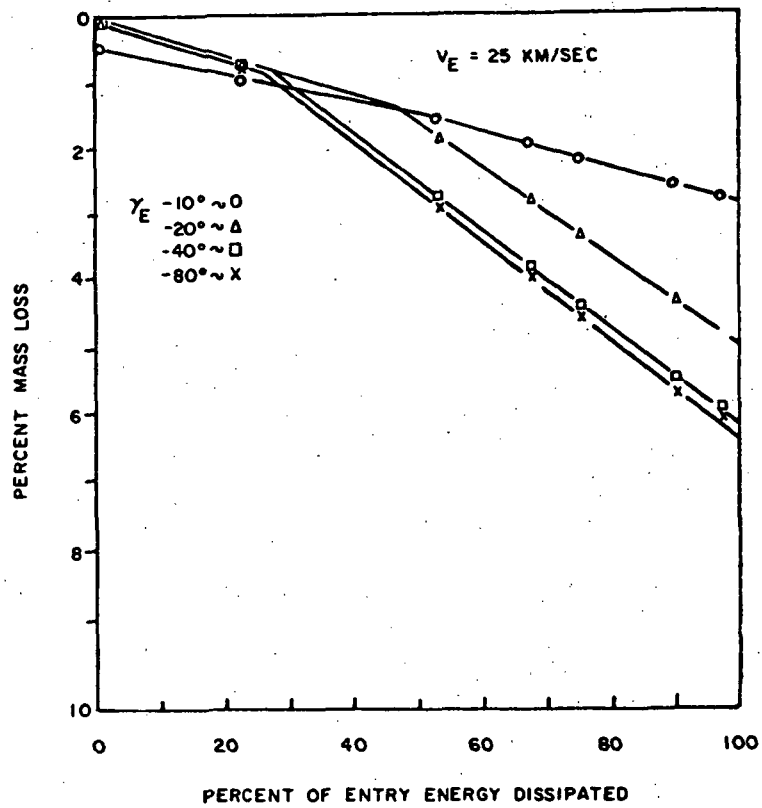


FIGURE 5. MASS LOSS AND ACCELERATION DURING ATMOSPHERIC ENTRY AT NEPTUNE (1981 GT)

slope of these curves for the steeper entry cases is due to the onset of turbulent flow. Although the gravitational parameters and the sizes of the two planets are similar, the scale height of the Neptune atmosphere is less than half that of Uranus (because Neptune is colder), and this accounts for the higher peak acceleration levels experienced during Neptune entries as compared with those into the atmosphere of Uranus.

Specific entry points are next chosen using the parametrized data of Figures 6, 7 and 8, which together describe the four mission possibilities. Figure 6 (Uranus/JUN 1979) will be described in detail; the other two figures are completely analogous to it. Each individual section of Figure 6 is plotted using inertial (i.e. non-rotating) longitude as the abscissa and latitude as the ordinate\*. The lower left graph shows the spacecraft ground track, the terminator, and potential probe paths after entry. In all cases, the probe enters to the west (left) of the spacecraft ground track, drifts toward the track, and crosses the track just as the spacecraft passes overhead. Thus, the choice of an entry point location implies the choice of an entry time as well. For example, if

$$t_{s/c} = \text{time of spacecraft flyover of probe track (hours before periapse)} = - 0.7 \text{ hr.}$$

$$t_p' = \text{time of probe entry (hours before intersection of probe path with ground track)} = - 0.45 \text{ hr.}$$

then

$$\begin{aligned} t_p &= \text{time of probe entry (hours before periapse)} \\ &= t_p' + t_{s/c} = - 1.15 \text{ hr.} \end{aligned}$$

\*Note that the latitude scale in Figure 7 is different from that in Figures 6 and 8.

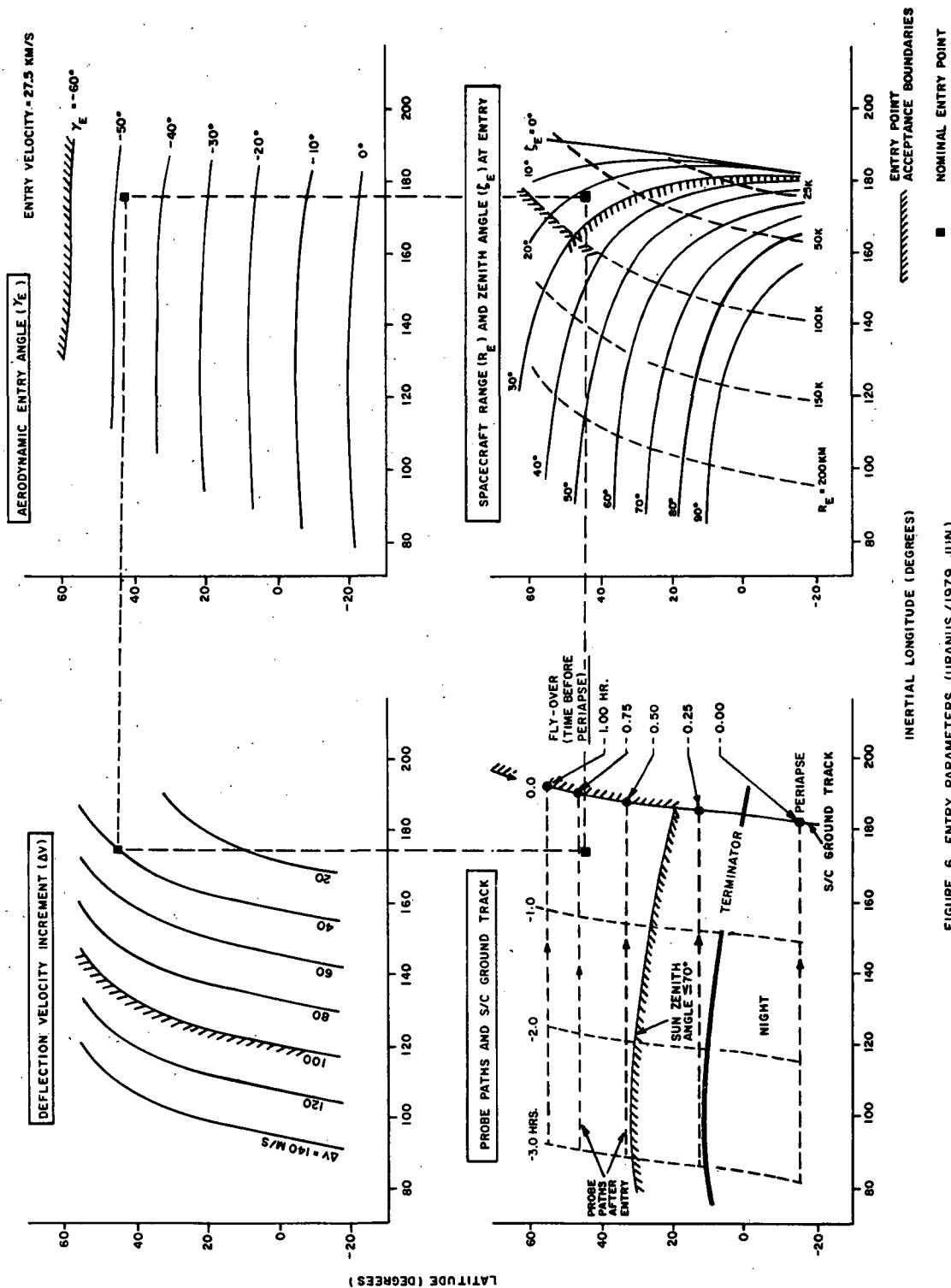


FIGURE 6. ENTRY PARAMETERS (URANUS/1979 JUN)

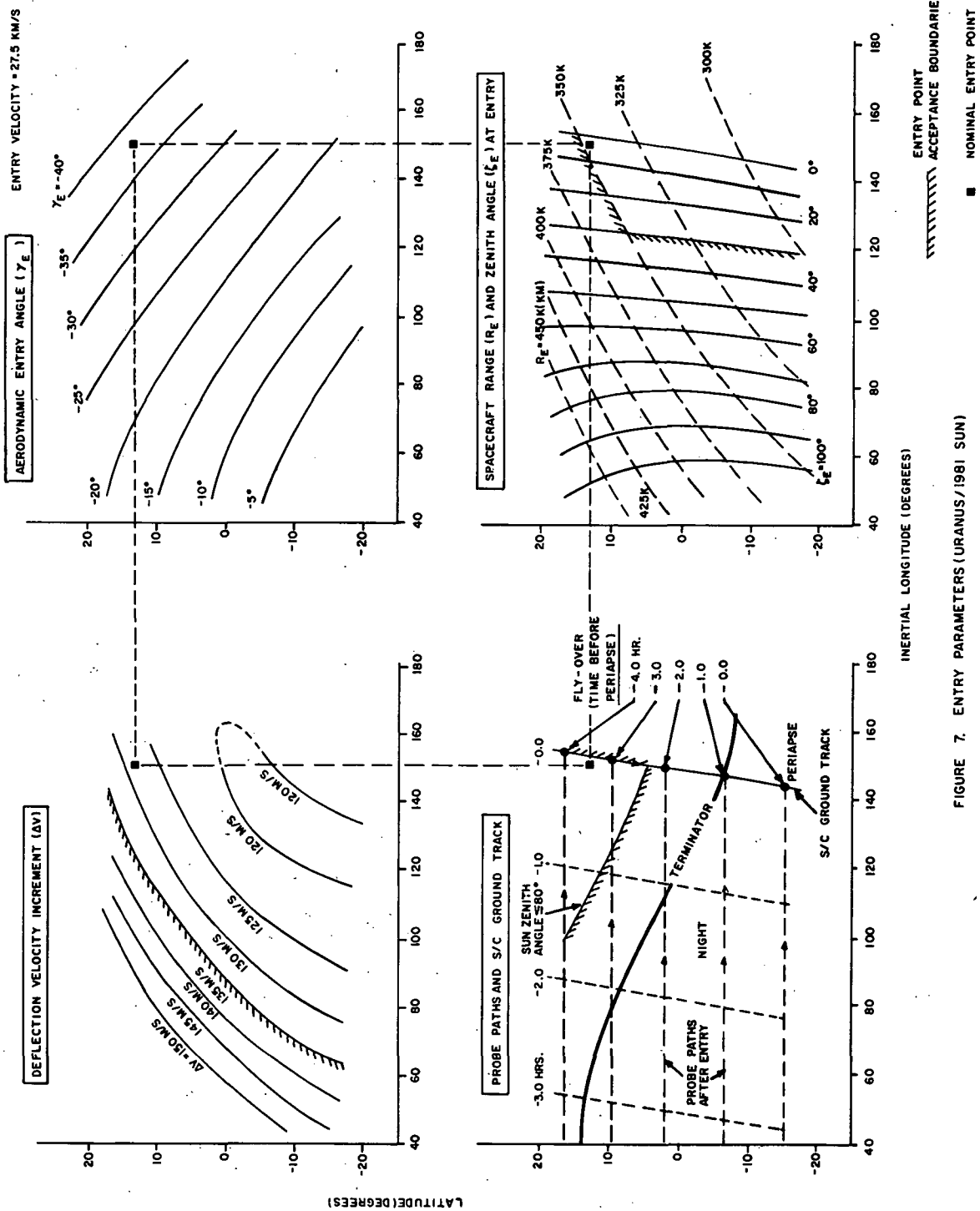


FIGURE 7. ENTRY PARAMETERS (URANUS/1981 SUN)

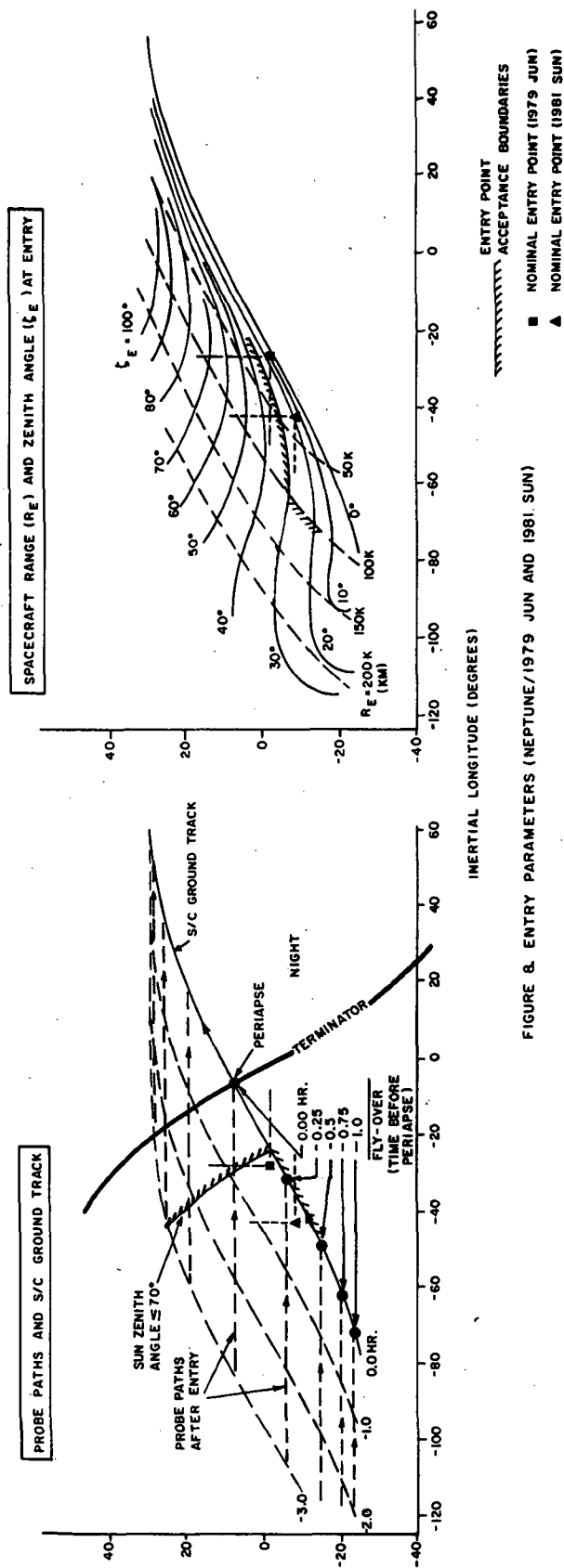
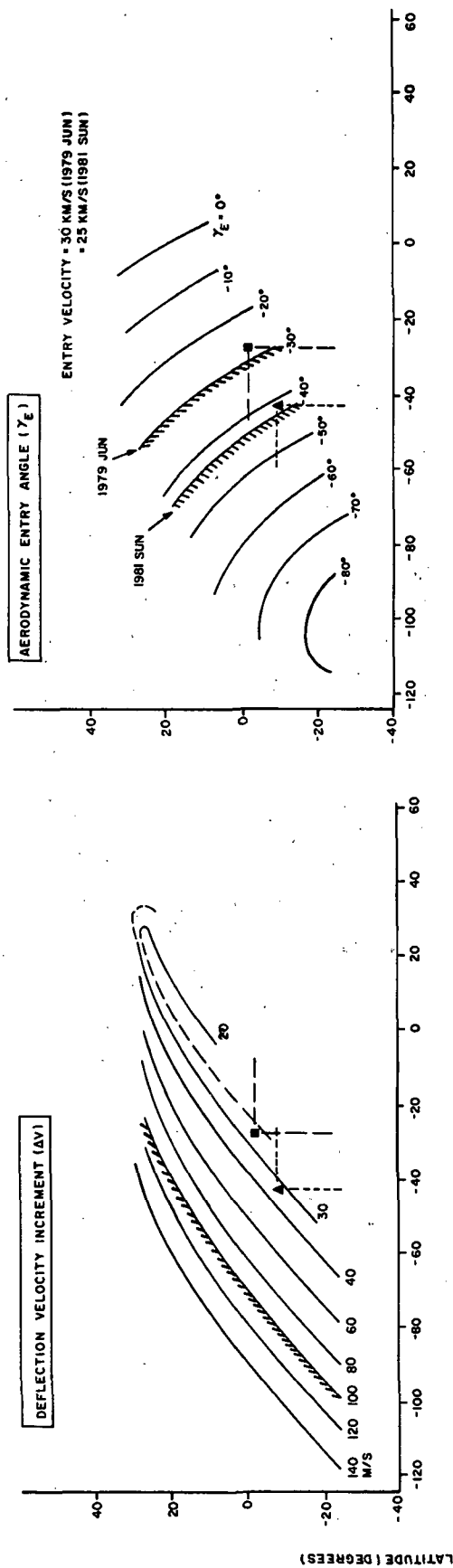


FIGURE 8. ENTRY PARAMETERS (NEPTUNE/1979 JUN AND 1981 SUN)



If the approach trajectory, deflection time, entry point location, and entry time are specified, the other entry parameters - deflection velocity increment, aerodynamic entry angle, and spacecraft range and zenith angle at entry - are determined. These quantities are plotted versus entry point location on the other parts of Figure 6.

For a successful entry, each of these parameters must be kept within certain bounds. Although these are not really sharp boundaries, we have considered them as such for simplicity and clarity. These "entry point acceptance boundaries" are shown using hatched lines in Figure 6, and represent these constraints:\*

Lower Left: (1) "S/C ground track". Entry to the west (left) of the spacecraft (S/C) ground track ensures that the S/C will fly over the probe during descent, which is desirable for effective data transmission throughout descent.

(2) "Sun zenith angle  $\leq 70^\circ$ ". This constraint ensures that the sun will be high enough in the sky to enable meaningful photometry measurements to be performed during descent. The constraint requires that the probe not enter too near the terminator, where atmospheric attenuation of solar radiation would be prohibitive.

Upper Left: (3) "Deflection Velocity Increment  $\leq 100$  m/s".

This constraint is imposed by size and weight considerations of the deflection propulsion system.

---

\* These constraints were not derived from extensive analysis and are meant to be merely typical. By overlaying a piece of vellum paper on Figures 6, 7 or 8, the reader can readily construct allowed entry regions corresponding to other constraints, using the parametric procedure described in this section.

Upper Right: (4) "Absolute Value of Aerodynamic Entry Angle  $= |\gamma_E| < 60^\circ$ ". This is based on the constraint that the maximum entry acceleration be  $\leq 600$  g's, to avoid damage to the probe and its contents.\* The constraint on entry angle is derived from Figure 3, from which it is evident that, for greater values of  $\gamma_E$ , entry accelerations are too high.

Lower Right: (5) "Spacecraft Range at Entry  $\leq 100K$  km". Data are transmitted continuously during descent. The constraint on range at entry comes from considerations of transmitter power.

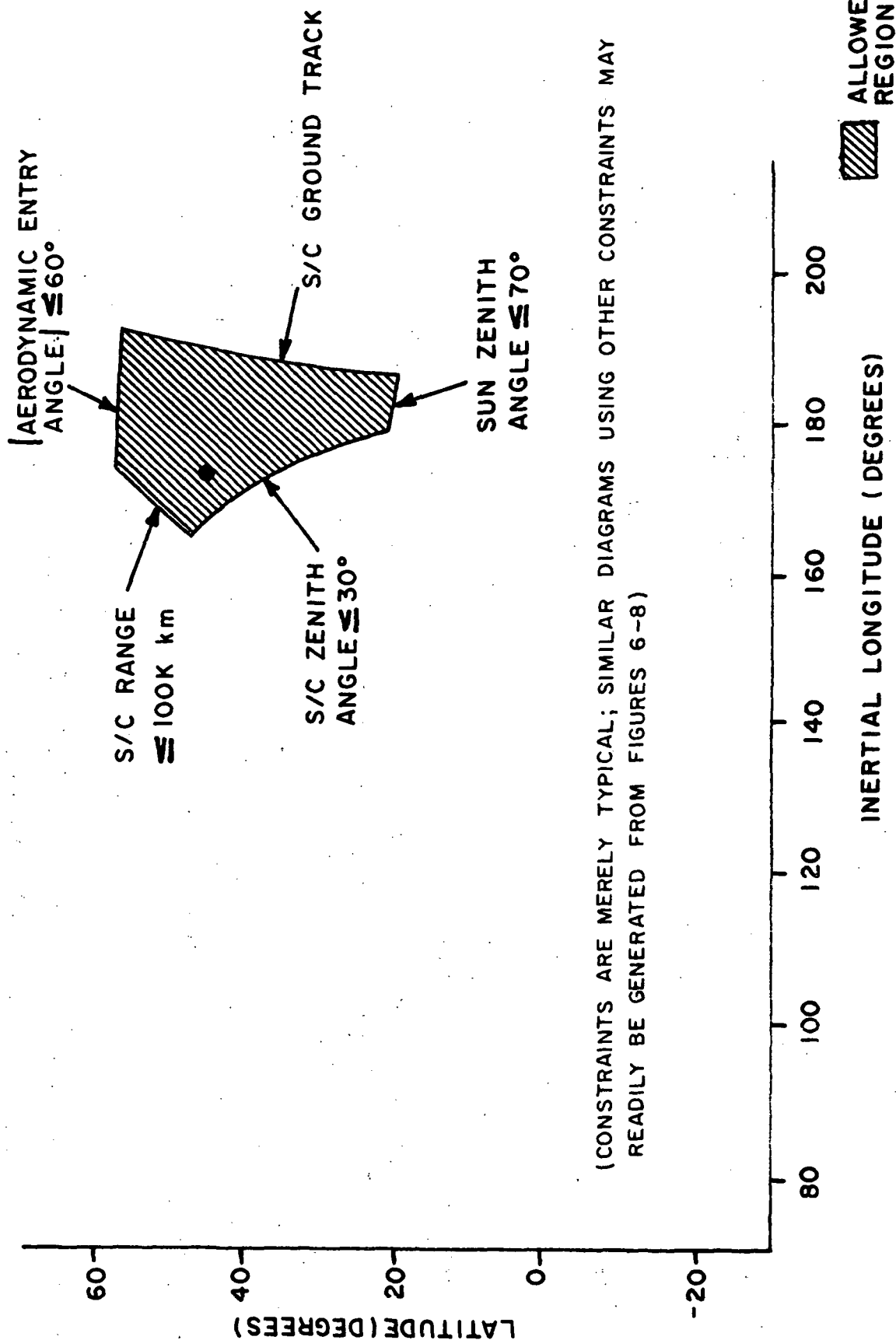
(6) "Spacecraft Zenith Angle at Entry  $\leq 30^\circ$ ". The radio link between the probe and spacecraft is attenuated by the atmosphere. The greater the spacecraft zenith angle, the greater is this attenuation. Thus this constraint also arises from considerations of transmitter power.

When all these limiting constraints are applied together, only a small locus of points is left over for the allowed region of entry. These allowed regions are shown for the four mission cases in Figures 9 through 12.\*\* The allowed region is quite large for Uranus/1979 JUN, somewhat smaller for Uranus/1981 SUN

---

\* This is perhaps a conservative constraint. Jupiter probes are designed for  $\sim 1000$  g's deceleration. However, it may not be necessary to design for such high g-loads for Uranus-Neptune entry. Also, from the parametric procedure described herein, allowed entry regions for 1000 or more g's may readily be determined.

\*\* With respect to Neptune, although the entry parameters for both opportunities are displayed on a single graph (Figure 8), the entry velocities are different: 30 km/sec for 1979 JUN, and 25 km/sec for 1981 SUN. This implies different entry acceleration profiles and different constraints on entry angle for the two opportunities (see upper right section of Figure 8). Therefore the two opportunities have different allowed regions of entry.



(CONSTRAINTS ARE MERELY TYPICAL; SIMILAR DIAGRAMS USING OTHER CONSTRAINTS MAY READILY BE GENERATED FROM FIGURES 6-8)

FIGURE.9. ALLOWED REGION OF ENTRY (URANUS/1979 JUN)  
 (NON-RESTRICTIVE CONSTRAINTS NOT SHOWN)

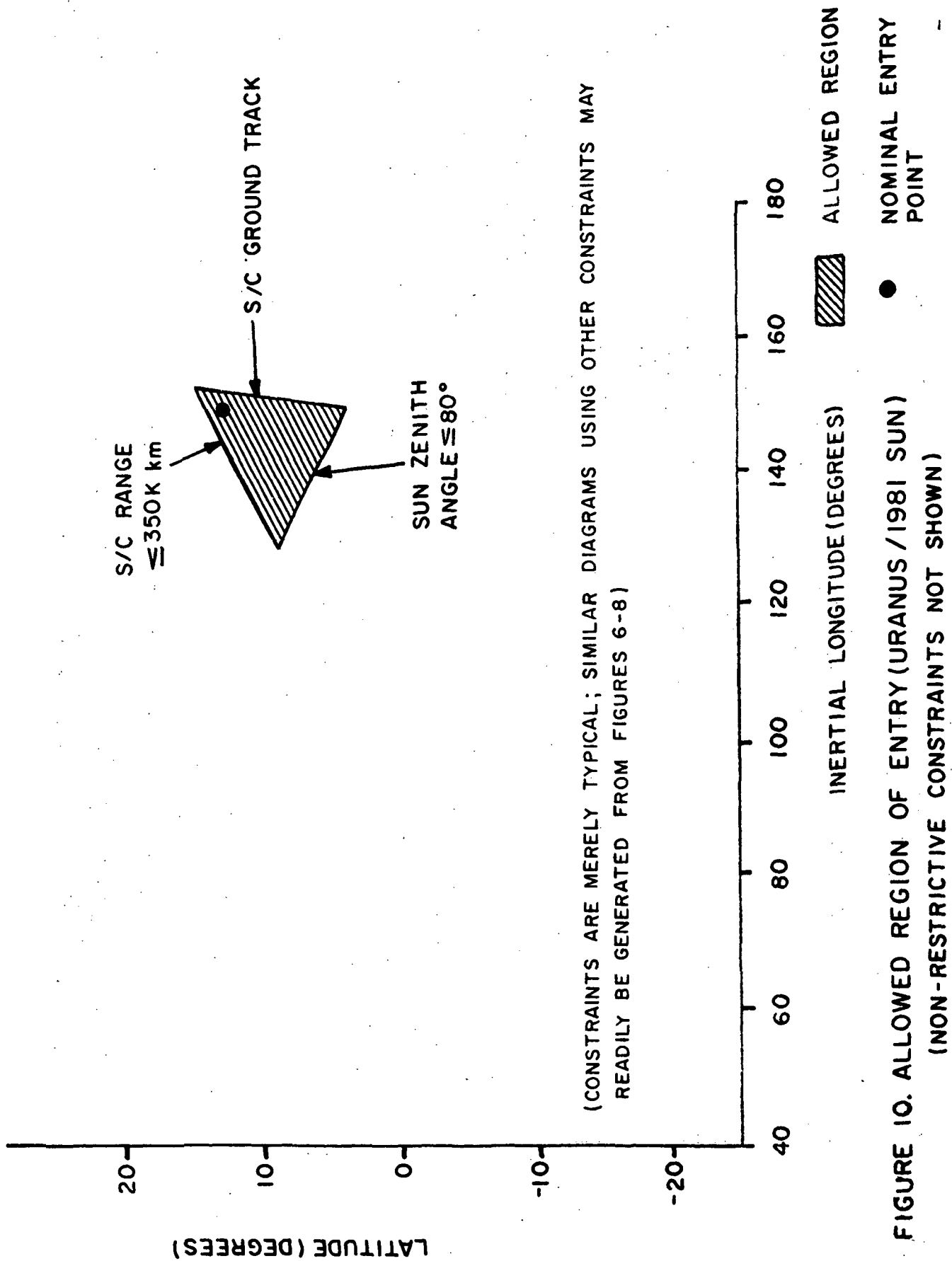


FIGURE 10. ALLOWED REGION OF ENTRY (URANUS/1981 SUN)  
 (NON-RESTRICTIVE CONSTRAINTS NOT SHOWN)

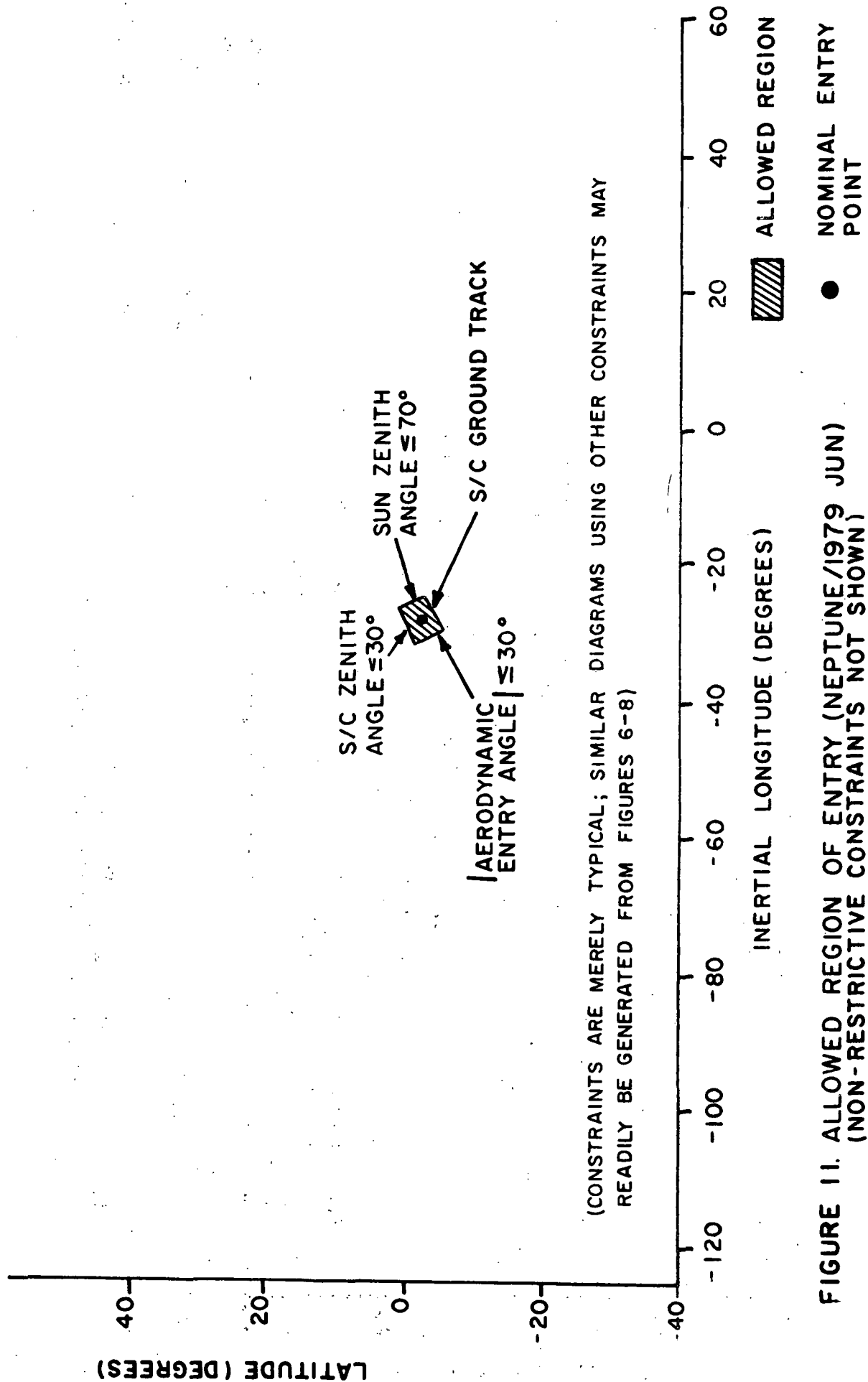


FIGURE 11. ALLOWED REGION OF ENTRY (NEPTUNE/1979 JUN)  
(NON-RESTRICTIVE CONSTRAINTS NOT SHOWN)

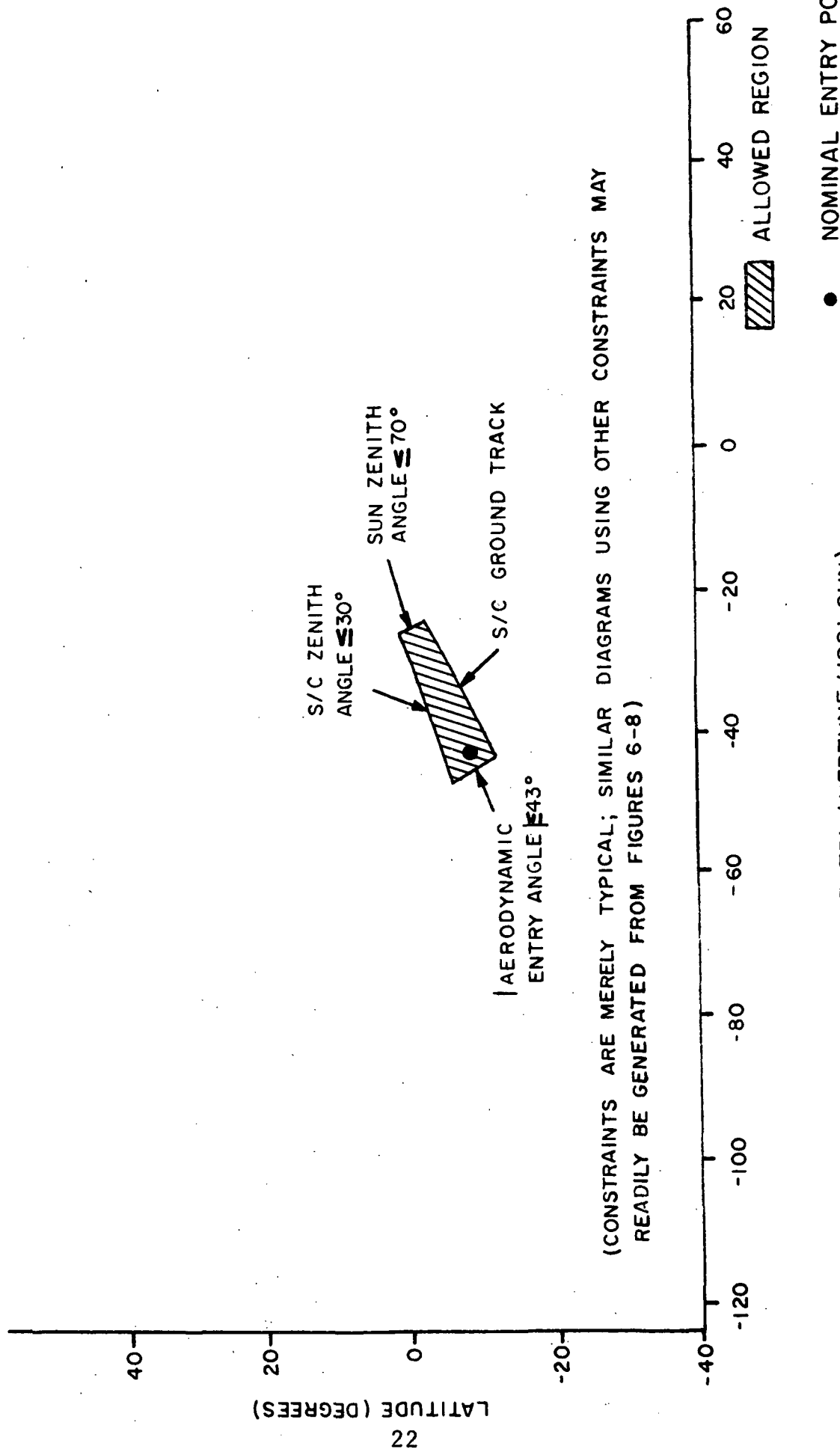


FIGURE 12. ALLOWED REGION OF ENTRY (NEPTUNE/1981 SUN)  
(NON-RESTRICTIVE CONSTRAINTS NOT SHOWN)

and Neptune/1981 SUN, and very small for Neptune/1979 JUN. All the constraints for the four mission cases are summarized in Table 2. From this table and Figures 9 to 12, it may be seen that not every constraint acts as a restriction on the allowed region of entry. It should also be noted that the constraints on the Uranus/1981 SUN opportunity had to be made less severe in order to yield any allowed entry points at all. This situation exists because the opportunity is basically less desirable than the 1979 JUN opportunity, due to the large periapse radius at Uranus.

Within the allowed regions of entry, attempts were made to optimize the choice of entry points. For Uranus/1979 JUN, the entry point was chosen to be fairly far from the terminator, so that the sun zenith angle would be fairly small and good photometry could be performed. An entry latitude of  $45^\circ$  was chosen on the assumption that latitudes further north might be less representative of the planet as a whole, and thus of less scientific interest. Also, the entry point was chosen such that the spacecraft would fly over the probe after the latter had been descending for 30 minutes and had reached 10 bars pressure; thus data transmission at the end of the mission would occur when the spacecraft was closest. For Uranus/1981 SUN, the prime consideration was to choose the entry point so as to minimize the sun zenith angle and improve the quality of the photometry; even so, this angle must be  $\sim 70^\circ$ . For Neptune/1979 JUN, the allowed region of entry is so small that it essentially determines a single allowed entry point. For Neptune/1981 SUN, again the sun zenith angle was minimized to equal  $\sim 50^\circ$ .

The nominal entry points have been entered on Figures 6 - 8. On each figure, because of the way the four individual graphs are plotted with respect to each other, the four representations of an entry point are located at the four corners of a rectangle, as indicated by the large dashed rectangles on these figures.



TABLE 2

## TYPICAL CONSTRAINTS ON ENTRY PARAMETERS

	Uranus/ 1979 JUN	Uranus/ 1981 SUN	Neptune/ 1979 JUN	Neptune/ 1981 JUN
Deflection Velocity Increment $\leq$	100 m/s*	135 m/s*	100 m/s*	100 m/s*
Sun Zenith Angle $\leq$	70°	80°	70°	70°
Entry Angle  $\leq$	60°	60°*	30°	43°
S/C Zenith Angle $\leq$	30°	30°*	30°	30°
S/C Range $\leq$	100 K km	350 K km	100 K km*	100 K km*
S/C Ground Track [Probe Path Intersects?] Yes	Yes	Yes	Yes	Yes
Chosen Entry Point (Inertial longitude; latitude)	173°, +45°	150°, +12°	-29°, -2°	-43°, -7°

\* Does not restrict allowed region of entry

Regardless of what entry point is chosen, the four representations still form the corners of a rectangle of the same size and shape. This fact makes it extremely simple to examine the consequences of a change in entry point. The reader may verify this for himself by taking a piece of vellum paper and tracing one of the dashed rectangles. Then, if the lower left corner of this rectangle is placed at any new entry point on the lower left graph, and if the rectangle is not rotated, the other corners will represent the entry point on the other three graphs, and will immediately yield the new values of the parameters plotted on them.

The entry deceleration profiles are shown in Figures 13 through 15. The trajectory profiles show aerodynamic velocity as a function of atmospheric pressure. During the early portion of the atmospheric entry, the curves are approximately straight lines. As velocity decreases, the profiles become asymptotic to the curves of constant dynamic pressure, which correspond to equilibrium between probe weight and aerodynamic drag as the probe descends vertically. As mentioned previously, the equilibrium curves are calculated for a ballistic coefficient of  $B = 150 \text{ kg/m}^2$ . It can be seen that, except for very steep entry angles (i.e.,  $|\gamma_E| > 40^\circ$ ), the probe velocity decreases to a Mach number of less than 0.6 before the probe reaches 0.1 atmospheres. This suggests that the entry aeroshell configuration will slow the vehicle adequately so that staging to the final descent configuration can occur at subsonic velocity, and before the probe descends to 0.1 atmospheres (desirable for scientific reasons). This eliminates the requirement for supplementary hypersonic drag devices.

### 2.3 Descent

As we have seen, the descent time cannot exceed  $\sim 30$  minutes, because of constraints on the probe-to-spacecraft line of sight. Furthermore, it is necessary that the probe descend to at least 10 bars, for scientific reasons. These two constraints were met

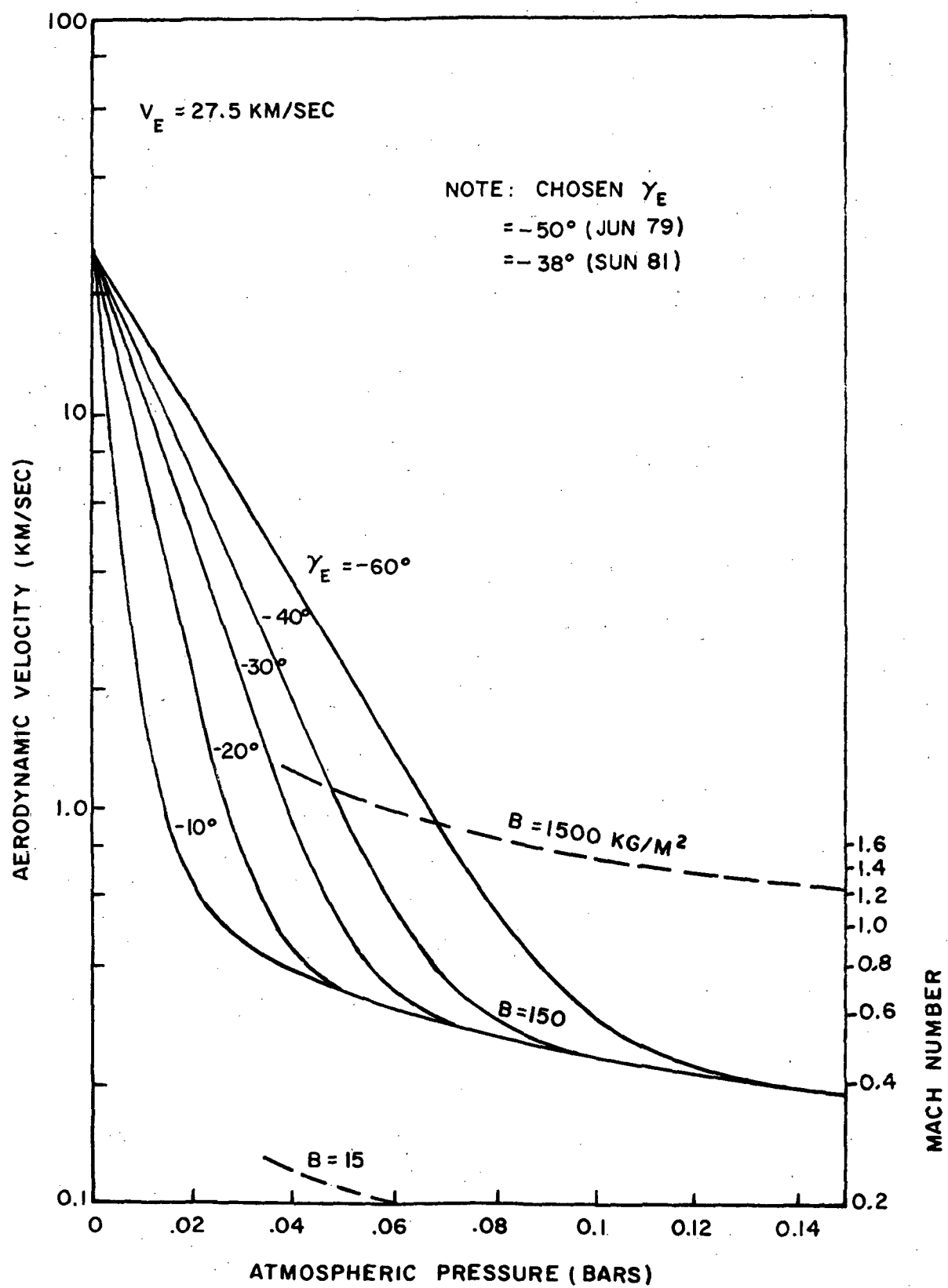


FIGURE 13. ENTRY PROFILE : URANUS/1979 JUN, 1981 SUN

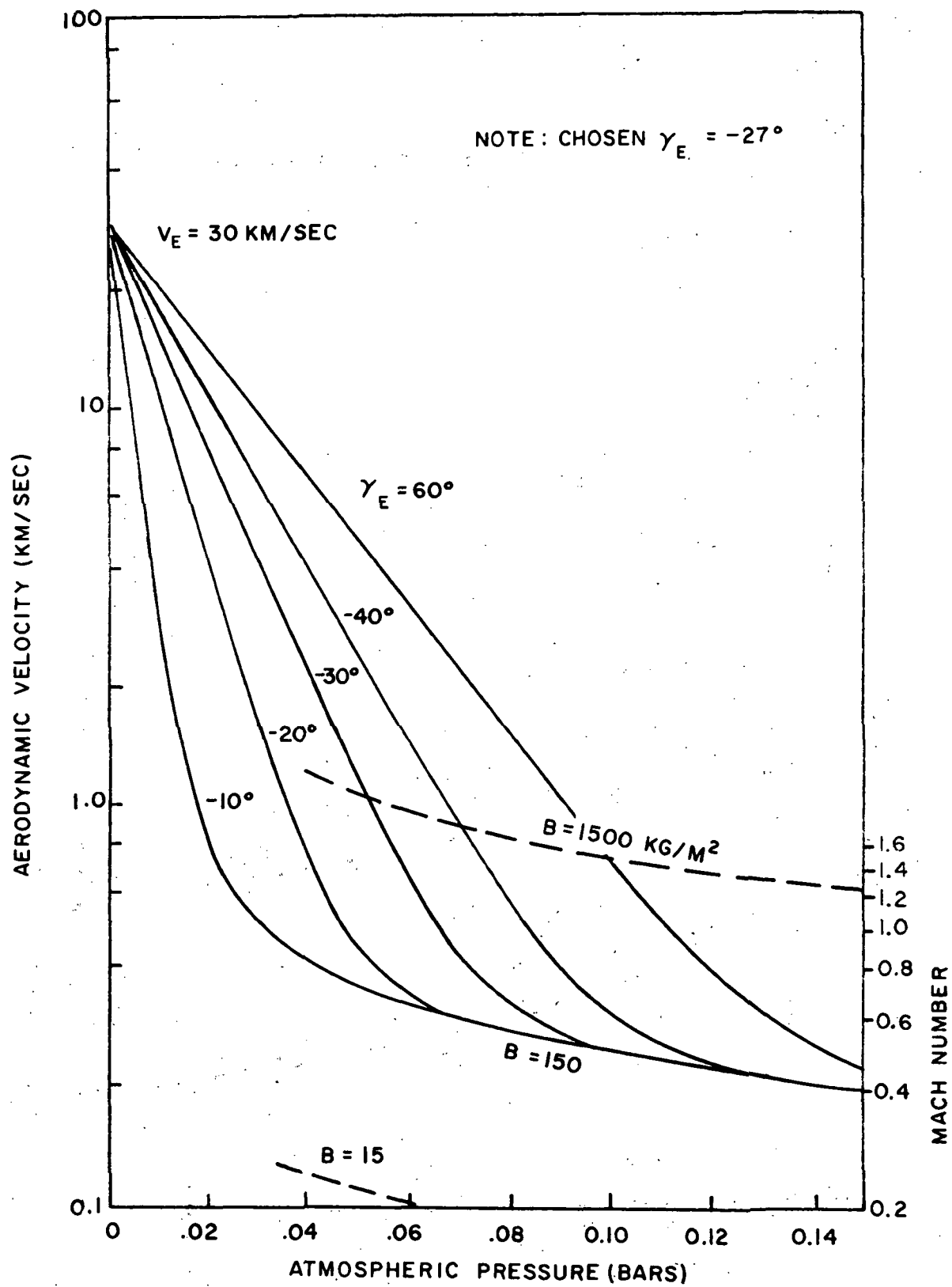


FIGURE 14. ENTRY PROFILE: NEPTUNE / 1979 JUN

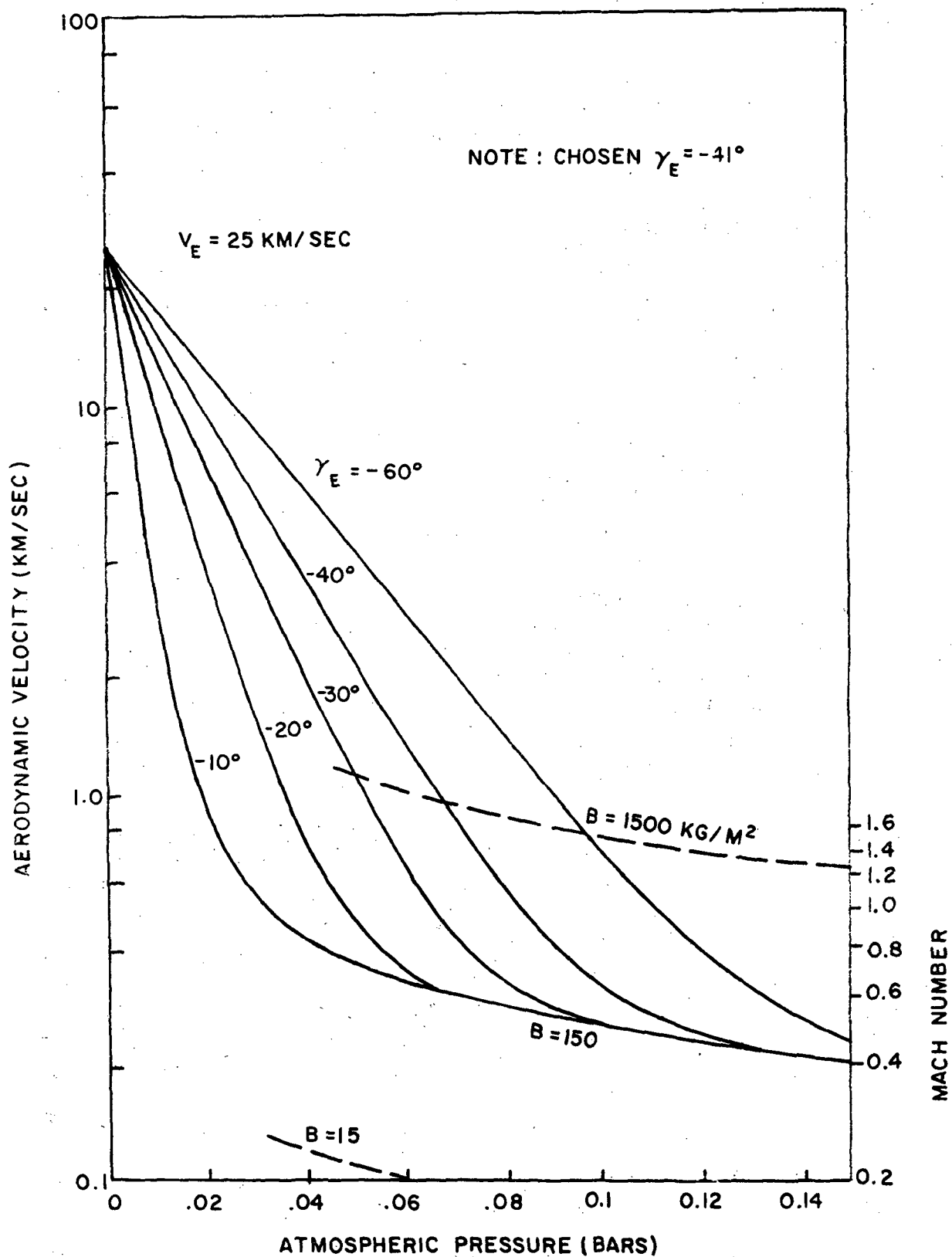


FIGURE 15. ENTRY PROFILE : NEPTUNE / 1981 SUN

by choosing appropriate ballistic coefficients. The effectiveness of various ballistic coefficients in penetrating the atmospheres of Uranus and Neptune is shown in Figures 16 and 17. From these curves, we chose descent ballistic coefficients (B) for Uranus and Neptune of  $200 \text{ kg/m}^2$  and  $55 \text{ kg/m}^2$ , respectively. For Uranus, B(descent) is slightly greater than B(entry), whereas for Neptune it is less. Therefore, on Neptune, a parachute must be attached during descent, but for Uranus this must not occur. Figures 18 and 19 show the descent profiles for Uranus and Neptune, derived from Figures 16 and 17. For Neptune the velocity after aeroshell-jettison is smaller than before, whereas for Uranus it is greater. For both planets, the aeroshell-payload separation occurs at Mach 0.6, which is shortly before the pressure equals 0.1 bars.

During descent on Uranus, even though a parachute is not used, the probe is nevertheless stabilized in zenith angle. Its conical shape must be aerodynamically designed so that its axis of symmetry remains vertical, i.e. it does not tumble. However, the probe is not stabilized in azimuth; it rotates about its axis of symmetry during descent at a nominal rate.

The basic parameters relating to deployment, entry, and descent are summarized in Table 3.

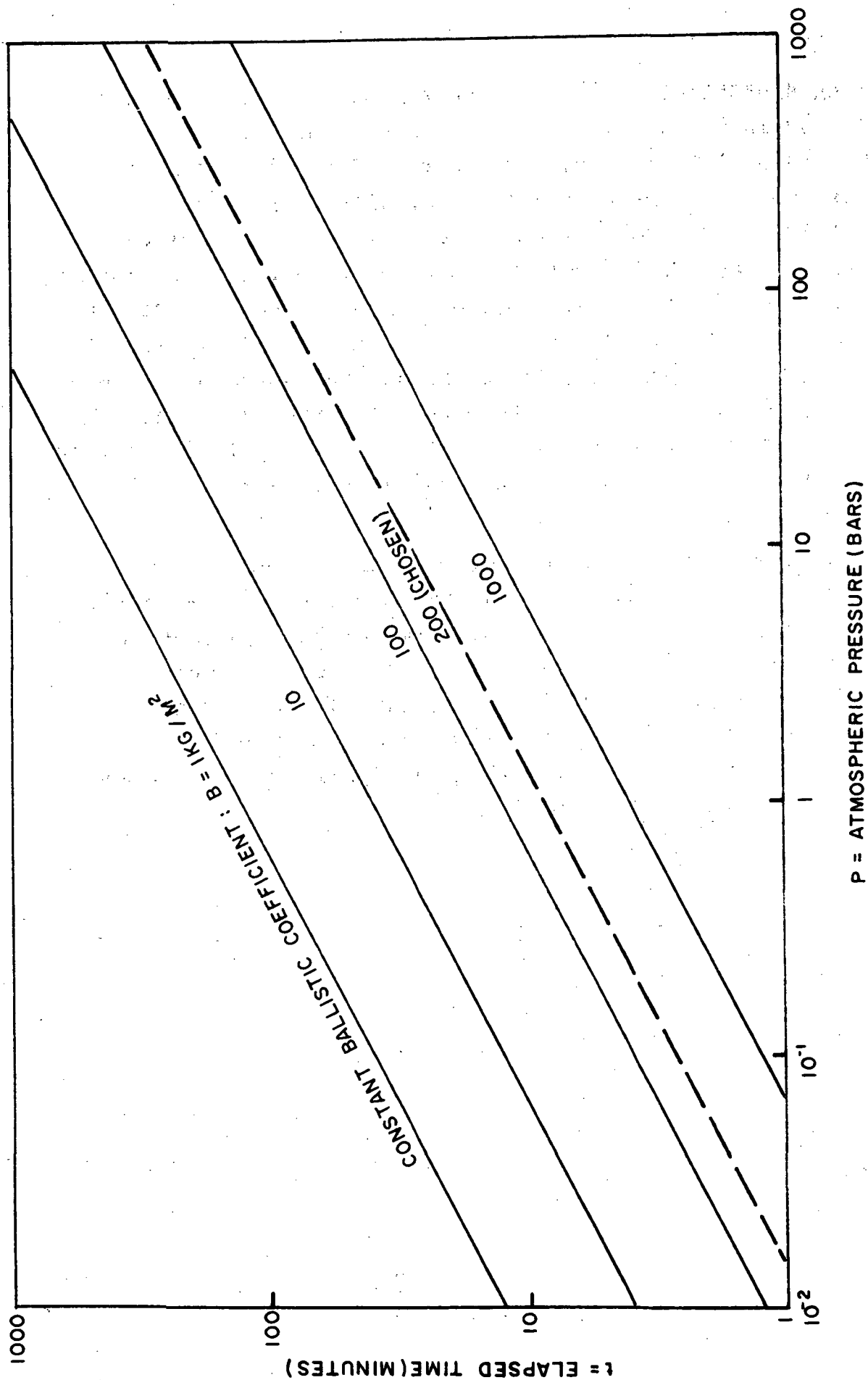


FIGURE 16. EQUILIBRIUM VERTICAL DESCENT AT URANUS  
 FOR A GIVEN  $B$ , THE DESCENT TIME BETWEEN ANY  $P_1$  AND  $P_2$  IS THE CORRESPONDING  
 INTERVAL  $t_2 - t_1$ .

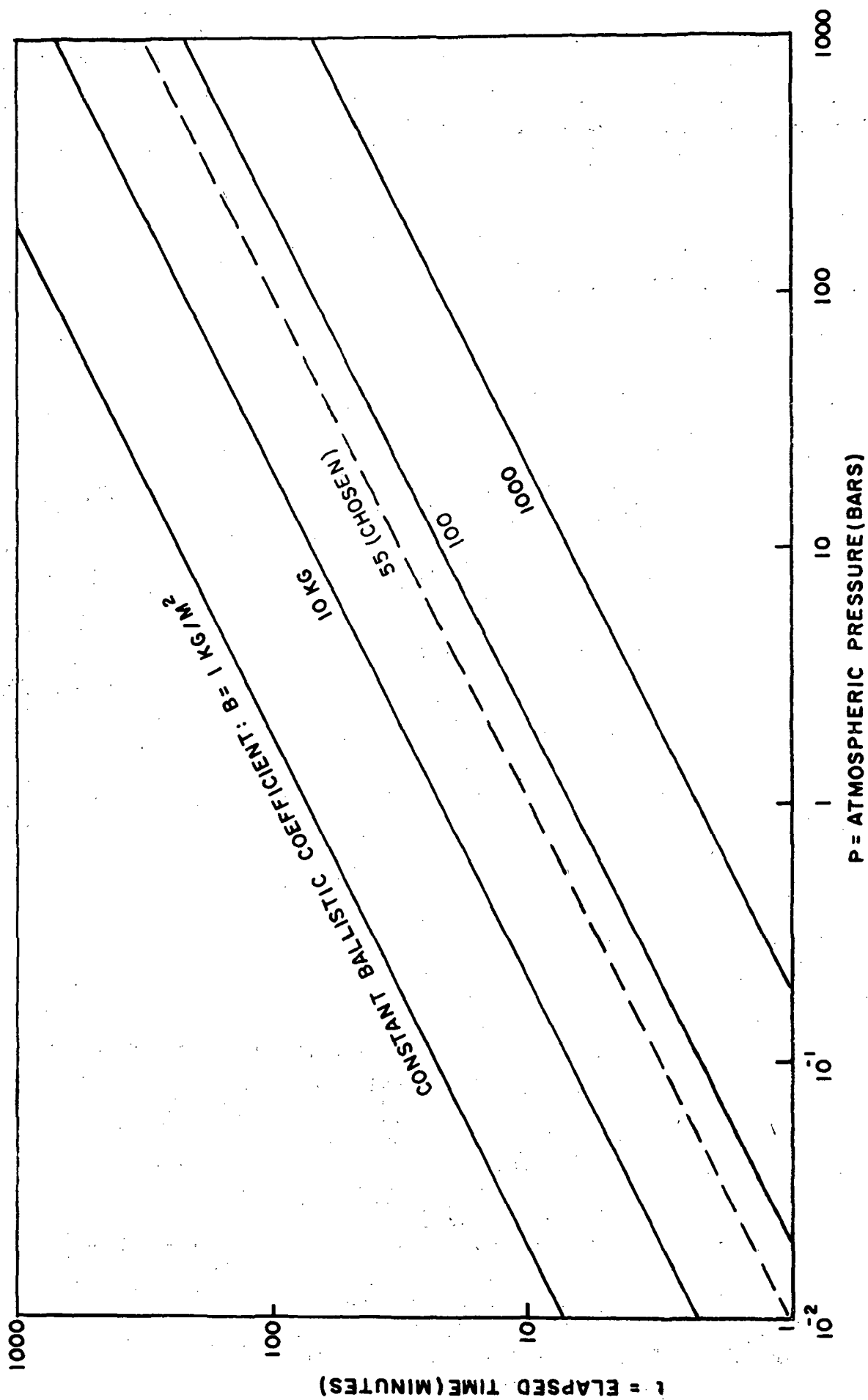


FIGURE 17 EQUILIBRIUM VERTICAL DESCENT AT NEPTUNE  
FOR A GIVEN  $B$ , THE DESCENT TIME BETWEEN ANY  $P_1$  AND  $P_2$  IS THE CORRESPONDING  
INTERVAL  $t_2 - t_1$



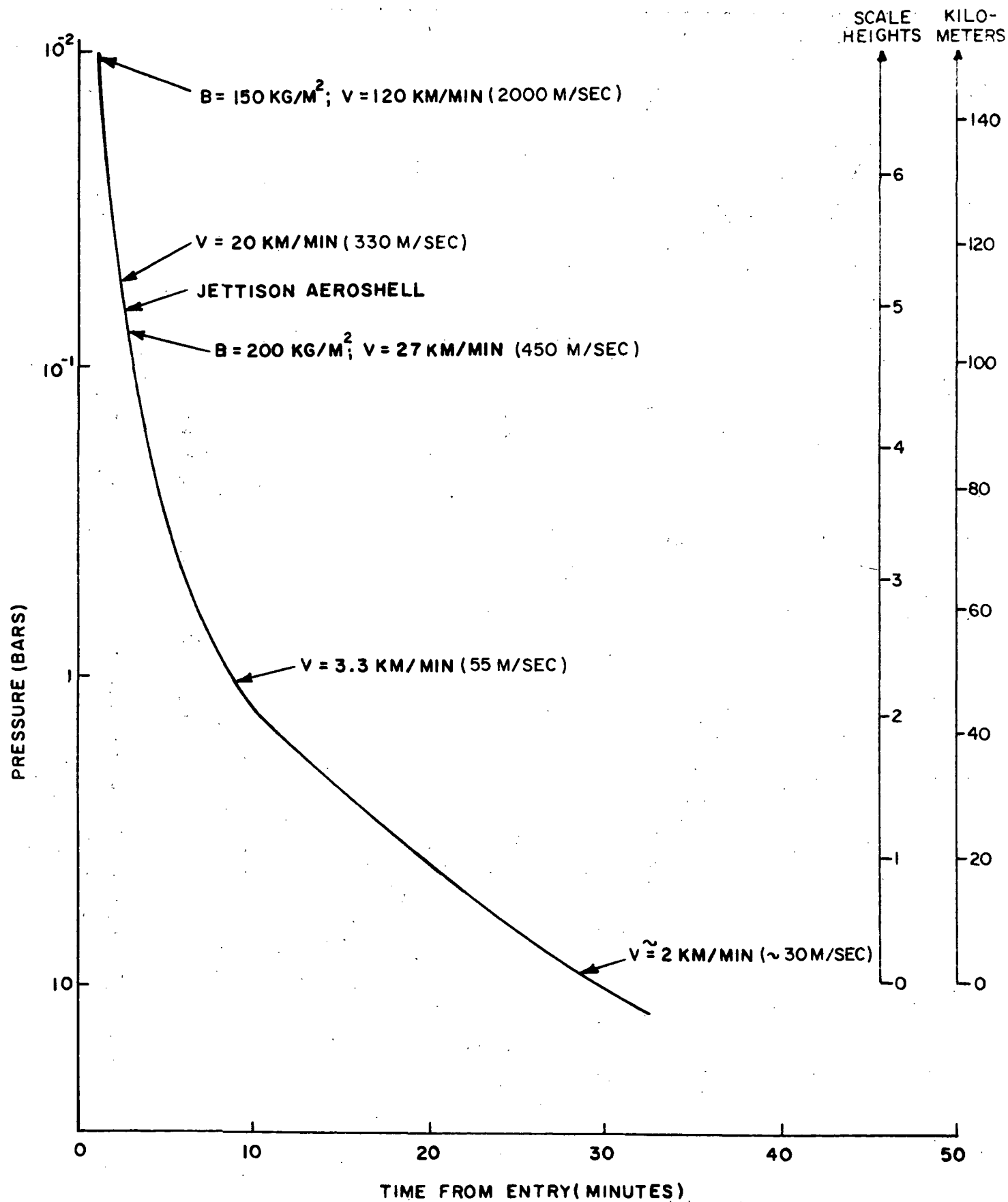


FIGURE 18. DESCENT PROFILE AT URANUS

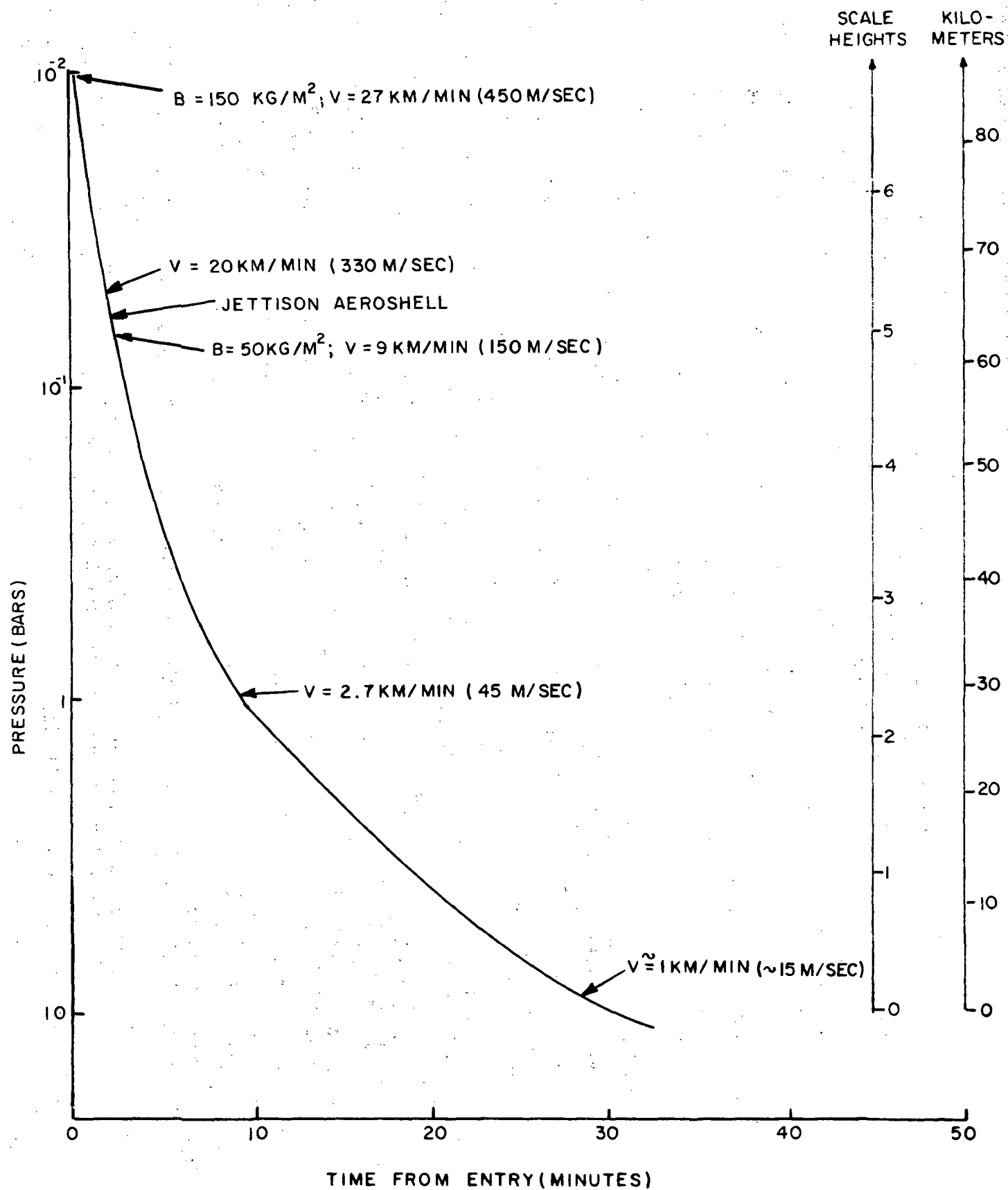


FIGURE 19. DESCENT PROFILE AT NEPTUNE

TABLE 3

## ENTRY AND DESCENT PARAMETERS FOR NOMINAL ENTRY POINTS

	Uranus		Neptune	
	1979 JUN	1981 SUN	1979 JUN	1981 SUN
Periapse Radius of Parent Spacecraft	1.63 p.r.	12.77 p.r.	2.0 <sup>a</sup> p.r.	2.0 <sup>a</sup> p.r.
Deflection Time	- 15 days	- 15 days	- 15 days	- 15 days
Deflection Velocity Increment	40 m/s	128 m/s	~ 23 m/s	33 m/s
Entry Point Location <sup>b</sup>	173°, +45°	150°, +12°	-29°, -2°	-43°, -7°
Entry Time	-1.15 hrs	-3.5 hrs	-0.4 hrs	-0.7 hrs
Entry Velocity	27.5 km/s	27.5 km/s	30 km/s	25 km/s
Entry Angle	-50°	-38°	-27°	-41°
S/C Range at Entry	80 K km	345 K km	~ 20 K km	40 K km
S/C Zenith Angle at Entry	23°	3°	10°-20°	~ 20°
Sun Zenith Angle at Entry	42°	72°	67°	50°
Maximum Deceleration	475 g's	550 g's	380 g's	580 g's
Entry Ballistic Coefficient	150 kg/m <sup>2</sup>	150 kg/m <sup>2</sup>	150 kg/m <sup>2</sup>	150 kg/m <sup>2</sup>
Descent Ballistic Coefficient	200 kg/m <sup>2</sup>	200 kg/m <sup>2</sup>	55 kg/m <sup>2</sup>	55 kg/m <sup>2</sup>
Scale Height	21.8 km	21.8 km	12.6 km	12.6 km
Initial Speed of Descent (0.1 bars)	27 km/min	27 km/min	9 km/min	9 km/min
Final Speed of Descent (10 bars)	2 km/min	2 km/min	1 km/min	1 km/min

<sup>a</sup>Periapse at Neptune may be chosen arbitrarily; we chose 2.0 planet radii as an effective compromise between range and line-of-sight motion.

<sup>b</sup>Inertial longitude, latitude.

### 3. SCIENTIFIC MEASUREMENTS

#### 3.1 Current Knowledge of the Atmospheres of Uranus and Neptune

Some basic facts about Uranus and Neptune are given in Table 4. A very complete review of current knowledge of these two planets has recently been given by Newburn and Gulkis (1971); this section draws freely from it.

The atmospheres of Uranus and Neptune are thought to consist primarily of hydrogen. Traces of methane definitely exist, and helium may or may not be present. Kuzmin and Losovskii (1971) claim evidence for traces of ammonia on Uranus. For the engineering portions of this study, we have assumed that the atmospheres consist essentially of 100% hydrogen, i.e., that  $\mu$  = mean molecular mass = 2.0 amu. The atmospheres are by no means isothermal (Trafton 1967). In fact, the temperature of the daylight side of Uranus is expected to vary significantly with the planet's location in its orbit. The rotation axis is practically in the orbit plane. Therefore, when the axis points toward the sun, the daylight side is somewhat warmer than when the axis is perpendicular to the sun's rays. Trafton obtained isothermal boundary temperatures ( $T$ ) of 47.5°K for Uranus and 37.4°K for Neptune. In the engineering portions of this study we make the extremely simple assumption that the atmospheres are isothermal at these temperatures. (More complicated models are discussed by Hunten (1971)). Also, these temperatures imply that (unlike Jupiter and Saturn) the planets Uranus and Neptune do not have internal heat sources, but are heated solely by sunlight.

Models of the atmospheres of Uranus and Neptune have recently been constructed by Belton, McElroy, and Price (1971) and by Prinn and Lewis (1972). Belton et al. conclude that the atmospheres are optically deep, composed of almost pure  $H_2$ , and

TABLE 4

## BASIC FACTS ABOUT URANUS AND NEPTUNE

	Uranus	Neptune
Semi-major axis <sup>a</sup>	19.18 AU	30.07 AU
Sidreal period of revolution	84.013 years	164.79 years
Radius <sup>b</sup>	25,300 km	23,600 km
Mass <sup>a</sup>	$8.67 \times 10^{28} \text{ g} (14.5 M_{\oplus})$	$10.30 \times 10^{28} \text{ g} (17.2 M_{\oplus})$
Density <sup>e</sup>	$1.27 \text{ g cm}^{-3}$	$1.87 \text{ g cm}^{-3}$
Surface Gravity <sup>e</sup> (g)	$905 \text{ cm s}^{-2}$	$1230 \text{ cm s}^{-2}$
Rotation Period <sup>c</sup>	$10.8 \pm 0.5 \text{ hrs}$	$15.8 \pm 1.0 \text{ hrs}$
Inclination of Equator to Orbit <sup>a</sup>	$97^{\circ} 55'$	$28^{\circ} 48'$
Isothermal Boundary Temperature (T) <sup>d</sup>	$47.5^{\circ} \text{K}$	$37.4^{\circ} \text{K}$
He/H <sub>2</sub> ratio by number (assumed)	0/100	0/100
Mean Molecular Mass <sup>e</sup> ( $\mu$ )	2.0 amu $= 3.34 \times 10^{-24} \text{ g}$	2.0 amu $= 3.34 \times 10^{-24} \text{ g}$
Scale height <sup>e,f</sup> (kT/ $\mu$ g)	21.8 km	12.6 km

<sup>a</sup>Allen 1963, p. 142<sup>b</sup>Belton, McElroy, and Price 1971<sup>c</sup>Newburn and Gulkis 1971<sup>d</sup>Trafton 1967<sup>e</sup>Calculated from other data in table.<sup>f</sup> $k$  = Boltzmann's constant =  $1.38 \times 10^{-16} \text{ erg } ^{\circ} \text{K}^{-1}$ 

IIT RESEARCH INSTITUTE

clear of cloud particles down to the effective level of penetration of visible sunlight (optical depth  $\sim 0.5$ ; pressure  $\sim 3$  bars). On the other hand, Prinn and Lewis conclude that a methane haze is present at  $\sim 0.1$  bars, and that Neptune may in addition have some condensed argon at about this level. From a study of the geometrical albedoes of both planets, Belton et al. determined planet radii which correspond to the levels at which the vertical Rayleigh/Raman scattering optical depth at  $5500 \text{ \AA}$  is 0.5. The radii obtained were 25,300 km and 23,600 km for Uranus and Neptune, respectively. These radii imply corresponding gravitational accelerations ( $g$ ) of  $905 \text{ cm s}^{-2}$  for Uranus and  $1230 \text{ cm s}^{-2}$  for Neptune. We have used these numbers and the aforementioned values of  $\mu$  and  $T$  to determine engineering parameters, including calculated scale heights (see Table 4) of 21.8 km for Uranus and 12.6 km for Neptune. These are the values assumed in the entry and descent analyses in this study. The uncertainty of these estimates is reinforced by results from a stellar occultation by Neptune. Freeman and Lynga (1970) measured a scale height of  $28.9 \pm 2.6$  km, whereas Kovalevsky and Link (1969) measured a scale height of 60 km.

The visible disks of Uranus and Neptune appear quite featureless. Some band structure has been reported at various times (Newburn and Gulkis 1971), but a recent photograph of Uranus by the Stratoscope II balloon-borne telescope revealed no structure (Sky and Telescope, 39, 367; June, 1970).

### 3.2 Scientific Instruments

We feel that the most important types of scientific measurements which should be made by atmospheric entry probes at Uranus and Neptune are, in order of importance, (1) measurements of atmospheric composition, (2) "equation of state" measurements, i.e. pressure, temperature, density and search for cloud particles, (3) "radiative transfer" measurements of transmitted solar radiation

and IR radiation emitted from the atmosphere. In this section, we shall discuss each of these measurements in some detail, explaining why they are important and what types of instruments should be used to perform them. Finally a specific scientific payload will be presented.

### 3.2.1 Composition Measurements

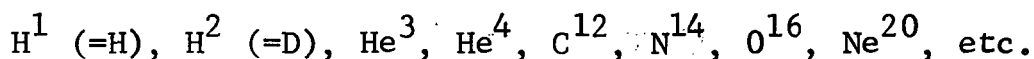
Although the atmospheres of the outer planets presumably differ in their dynamical properties (scale height, temperature, turbulence, convection, etc.), they appear to be quite similar in composition, consisting primarily of  $H_2$ , plus (possibly) some He, with smaller amounts of  $CH_4$  and  $NH_3$ . Furthermore, the abundances of the corresponding elements seem to be consistent with the solar abundances, and indeed with the cosmic abundances (Suess and Urey 1956). Therefore, it seems that these atmospheres are primordial and may contain valuable clues concerning the origin of the solar system, and perhaps even of the universe.\* For this reason atmospheric composition is considered to be a very valuable measurement, and the most important measurement for an atmospheric entry probe to any of the outer planets.

#### (1) Mass Spectrometer

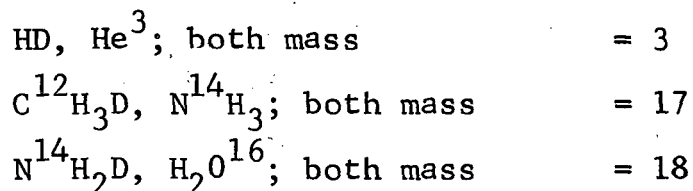
It is imperative to perform a series of composition analyses which are sensitive to isotopes. The best instrument for such analyses is a mass spectrometer. Either a quadrupole (Dawson et al. 1969) or an electrostatic-plus-magnetic analyzer (Nier and Hayden 1971) can provide good resolution of adjacent mass numbers for an extremely low instrument mass.

\* A major difference between "big-bang" and "steady-state" theories of the origin of the universe is that they predict significantly different values of the overall cosmic He/H ratio.

Table 5 shows, by mass number, possible species which may occur in the atmospheres of Uranus and Neptune. These correspond to the isotopes of greatest cosmic abundance, which are:



(Suess and Urey 1956).  $\text{F}^{18}$  is missing because it is not stable; otherwise HF would also be an atmospheric constituent. In the naturally-occurring atmosphere, no species of mass numbers 5-15 are expected. Furthermore, some mass ambiguities occur, for example:



The atmospheric gas sample must be ionized in preparation for its passage through the mass spectrometer. The usual method is to bombard the gas molecules with electrons, thereby knocking out electrons from the molecules and forming positive ions. Unfortunately, this procedure often breaks up the molecule itself to some extent. E.g. when  $\text{CH}_4$  is bombarded with 50 volt electrons, the relative abundances are:

<u>Species</u>	<u>M/e</u>	<u>Relative Abundance</u>
$\text{CH}_4$	16	100.0
$\text{CH}_3$	15	86.1
$\text{CH}_2$	14	16.3
CH	13	8.21
C	12	2.57
-	2	0.34
-	1	7.05



TABLE 5  
POSSIBLE CONSTITUENTS OF THE ATMOSPHERES  
OF URANUS AND NEPTUNE

Mass No.	Species	
1	(H <sup>1</sup> )	
2	H <sub>2</sub>	
3	HD, He <sup>3</sup>	
4	He <sup>4</sup>	
.		
.		
.		
16	C <sup>12</sup> H <sub>4</sub>	} Among Others
17	C <sup>12</sup> H <sub>3</sub> D, C <sup>13</sup> H <sub>4</sub> , N <sup>14</sup> H <sub>3</sub>	
18	N <sup>14</sup> H <sub>2</sub> D, N <sup>15</sup> H <sub>3</sub> , H <sub>2</sub> O <sup>16</sup>	
19	HDO <sup>16</sup> , H <sub>2</sub> O <sup>17</sup>	
20	H <sub>2</sub> O <sup>18</sup> , Ne <sup>20</sup>	
21	Ne <sup>21</sup>	
22	Ne <sup>22</sup>	
.		
.		
.		
Etc.		

(from NBS data sheets). Such a pattern is called a "cracking pattern". The problem of untangling the cracking patterns and measuring relative abundances in an unknown mixture of  $\text{CH}_4$ ,  $\text{NH}_3$ ,  $\text{H}_2\text{O}$ , etc. plus their singly-deuterated forms is of great importance and must be studied carefully as part of the design of any mass spectrometer for an outer planet entry probe.

One of the most difficult ambiguities arises in the measurement of the H:D and  $\text{He}^3:\text{He}^4$  ratios, which are of great importance to theories of solar system origin. At mass 3 one would expect not only  $\text{HD}^+$  and  $(\text{He}^3)^+$  but also  $\text{H}_3^+$ . Possibly one could employ negative ion mass spectroscopy (producing only  $\text{HD}^-$ , not  $\text{H}_3^-$  or  $(\text{He}^3)^-$ ) to resolve this ambiguity. A quadrupole mass spectrometer could readily be used to analyze both + and - ions with the same instrument (however, a magnetic sector instrument using a permanent magnet could not).

If hardware studies indicate that the ambiguities related to deuterium cannot be resolved using only the mass spectrometer, an additional instrument is necessary. A gas chromatograph was considered for this purpose, but this instrument takes 2 to 5 minutes to perform a measurement (AVCO 1971, Vol. II, p. 3-24) compared to as little as 0.5 seconds for a mass spectrometer. The former time was considered too excessive, considering the rapid descent rate required to reach 10 bars in 30 minutes. Instead, it was decided to choose a spectrophotometer to perform an independent measurement of the deuterium concentration.

## (2) H:D Photometer

The D:H ratio in outer planet atmospheres is estimated to lie between the theoretical value for the primitive solar nebula ( $\sim 10^{-5}$ ) and the present value for terrestrial water ( $\sim 1.5 \times 10^{-4}$ ).

Also, the C:H ratio in the atmospheres of Uranus and Neptune is believed to be somewhat higher than the solar value of  $\sim 3.5 \times 10^{-4}$  (Cameron 1972). We assume that essentially all of the deuterium is present as either HD or  $\text{CH}_3\text{D}$ . The ratio

$$r = \frac{(\text{CH}_3\text{D}/\text{CH}_4)}{(\text{HD}/\text{H}_2)}$$

is a strong function of temperature, increasing as temperature decreases. Specific values have been provided us by Cameron (1972, private communication). Values for  $r$ , D:H, and C:H then determine  $\text{CH}_3\text{D}:\text{D} = 1 - \text{HD}:\text{D}$ . We estimate that

$T = 150^\circ\text{K}$	$\text{CH}_3\text{D}:\text{D} < 10\%$
$T = 100^\circ\text{K}$	$\text{CH}_3\text{D}:\text{D} \sim 25\%$
$T = 50^\circ\text{K}$	$\text{CH}_3\text{D}:\text{D} \sim 50\%$

(all concentrations are by number).

To study absorption bands, a spectrophotometer on an entry probe would look directly at the sun. To study emission lines, an instrument would observe portions of the atmosphere fairly near the sun. In either case, the instrument would observe the atmosphere above the probe. If this atmosphere were approximately isothermal, data interpretation would be more straightforward. The models of Traftron (1967) indicate that, for Uranus and Neptune, the temperature of the upper atmosphere ( $P \lesssim 0.3$  bars) is  $\sim 40^\circ$  to  $50^\circ\text{K}$ , whereas that of the lower atmosphere ( $P \approx 0.3$  to 3 bars) steeply rises to at least  $90^\circ\text{K}$  (Neptune) or  $150^\circ\text{K}$  (Uranus). Therefore, the atmosphere above the probe would probably be approximately isothermal at  $\sim 50^\circ\text{K}$  for at least the first several minutes of descent.

We wish to use the spectroscopic method most appropriate for an atmosphere at this temperature.  $\text{CH}_3\text{D}$  and  $\text{HD}$  are expected to be present in approximately equal amounts.  $\text{CH}_3\text{D}$  could most readily be studied via its vibration-rotation absorption bands in the IR, whereas  $\text{HD}$  would have to be studied via its electronic lines in the UV (probably emission) (see Herzberg 1945, 1950). Since  $\text{CH}_3\text{D}$  absorption bands have been observed from Earth on Jupiter (Beer et al. 1972) and since AVCO recommended observation of a  $\text{CH}_3\text{D}$  absorption band for a Jupiter entry probe (AVCO 1971a), we also suggest observation of  $\text{CH}_3\text{D}$ . The relevant band occurs at  $\sim 2100\text{-}2200 \text{ cm}^{-1}$  ( $4.54\text{-}4.76 \text{ }\mu\text{m}$ ).

The probe is axially symmetric. Its axis remains approximately vertical during descent, although the probe rotates about the axis at some predetermined rate (a few rpm). During the short time of descent, the sun remains at approximately a constant zenith angle (this is especially true on Uranus, where the sun is practically above the north pole). An optical system collects sunlight from all azimuths and from an appropriate range of zenith angles. Five wavelength channels, each  $\sim 0.2 \text{ }\mu\text{m}$  wide, are used. The signal-to-noise ratio may be estimated as follows. The solar flux at  $4.6 \text{ }\mu\text{m}$  at Uranus and Neptune is

$$F_{\odot} (\text{Uranus}) = 1.8 \times 10^{-2} \text{ w m}^{-2} \text{ }\mu\text{m}^{-1}$$

$$F_{\odot} (\text{Neptune}) = 0.7 \times 10^{-2} \text{ w m}^{-2} \text{ }\mu\text{m}^{-1}$$

We assume

$$A = \text{acceptance area of optical system} = 10 \text{ cm}^2$$

$$\Delta\lambda = \text{channel width} = 0.2 \text{ }\mu\text{m}$$

$$\eta = \text{transmission of optical system} = 0.25$$

Then

$$\begin{aligned}\text{Signal} &= F_0 A \Delta\lambda \eta \\ &= 8.9 \times 10^{-7} \text{ watts (Uranus)} \\ &= 3.6 \times 10^{-7} \text{ watts (Neptune)}\end{aligned}$$

To compute the noise, we assume

$$\begin{aligned}A_d &= \text{area of IR detector} = (2 \text{ mm})^2 = 4 \times 10^{-6} \text{ m}^2 \\ \Delta f &= \text{electrical bandwidth} = 100 \text{ Hz} \\ D^* &= \text{figure of merit} = 10^9 \text{ cm Hz}^{\frac{1}{2}} \text{ watt}^{-1}.\end{aligned}$$

These figures are for an uncooled (290°K) PbSe detector (Santa Barbara Research Corporation, Goleta, Calif.; brochure). Then

$$\text{Noise} = \frac{A_d^{\frac{1}{2}} (\Delta f)^{\frac{1}{2}}}{D^*} = 2 \times 10^{-9} \text{ watts}.$$

The signal-to-noise ratio is 440 for Uranus, 180 for Neptune. Furthermore it can be improved by using an array of smaller detectors (smallest  $\cong .05$  mm), cooling the detector somewhat, or by more detailed optimization of the parameters above. Attenuation of the  $4.54 \mu\text{m}$  radiation by atmospheric  $\text{H}_2$  appears to be comparable to that for visible light (Belton et al. 1971, Fig. 9).

It is not possible to make a precise estimate of the strength of the absorption line versus total  $\text{CH}_3\text{D}$  above the probe, because precise curves of growth for  $\text{CH}_3\text{D}$  have not yet been published. However, these should be available soon. In any case such curves should be measured before a specific photometer is designed. The estimated amount of methane above

the level of penetration of visible light is  $\sim 3.5$  km - amagat for Uranus and  $\sim 6$  km - amagat for Neptune. This is much greater than the estimated amount on Jupiter:  $\sim 30$  m-amagat (Newburn and Gulkis 1971). Teifel and Kharitonova (1970)\* argue that this estimate may be too high by a factor of  $\sim 100$ . In any case, since  $\text{CH}_3\text{D}$  has been observed from Earth on Jupiter, it should be observable in-situ on Uranus and Neptune.

### 3.2.2 Equation of State Measurements

The equation of state of a perfect gas is

$$P = \frac{\rho}{\mu} kT,$$

where

$P$  = pressure

$\rho$  = density

$\mu$  = mean molecular mass

$k$  = Boltzmann's constant

$T$  = absolute temperature.

The entry probe is designed to survive only to about 10 bars pressure. The atmosphere doubtless behaves like a perfect gas at such pressures; however, it would be useful to confirm this. Therefore, it is desirable to measure all these variables - pressure, density, temperature, and mean molecular mass - directly, rather than estimating one or more from the perfect gas law.

---

\* As quoted in a draft JPL monograph on Uranus, Neptune and Pluto.

The measurement of temperature as a function of altitude,  $T(h)$ , is particularly important to the study of the dynamics of any atmosphere. One discusses the lapse rate:

$$\beta(h) = - \frac{dT}{dh} (h).$$

$\beta$  is positive if temperature decreases with altitude, as it does near the Earth's surface. A critical value of  $\beta$  is that which occurs in an adiabatic atmosphere:

$$\beta_a = \frac{\gamma-1}{\gamma} \frac{\mu g}{k},$$

where

$g$  = local gravitational constant  
 $\gamma$  = ratio of specific heats ( $C_p/C_v$ )  
 $= 1.4$  for a diatomic gas.

For example, taking  $\gamma = 1.4$ , we find

$$\beta_a (\text{Uranus}) = 0.63 \text{ } ^\circ\text{K/km}$$

$$\beta_a (\text{Neptune}) = 0.86 \text{ } ^\circ\text{K/km}.$$

The study of lapse rates and convection is fundamental to the study of planetary atmospheres. If  $\beta < \beta_a$ , the lapse rate is "subadiabatic", and no convection occurs. If  $\beta > \beta_a$ , the lapse rate is "superadiabatic", and convection occurs. (In practice, as soon as  $\beta$  tends to exceed  $\beta_a$ , convection acts to cancel this tendency and keep  $\beta \approx \beta_a$ .)

### (1) High -g Accelerometer

For engineering simplicity, it was decided that there would be no "windows" in the heat shield. Therefore, the only measurement during entry (as opposed to descent) is that of acceleration. This yields the extremely important information regarding the atmospheric density  $\rho(h)$  from the relation

$$\rho = \frac{2Ba_m}{v^2}$$

where

$a_m$  = measured acceleration

$B$  = ballistic coefficient

$v$  = velocity.

It is very important that the atmosphere be reconstructed from data measured on board the probe, i.e. that all measured quantities (composition, density, pressure, temperature, transmitted solar radiation, and emitted IR radiation) be determined eventually (after data analysis) as functions of relative altitude, and if possible absolute altitude. This can be accomplished by integrating the acceleration, which is determined from the accelerometers. The procedure is fairly complex but is well documented (e.g. see Swenson et al. 1971, Seiff 1968)\*. We specify a 3-axis high-g accelerometer similar to that proposed for Jupiter entry by AVCO (1971). The three components of acceleration are measured every two seconds during entry and the data are stored for transmission during descent.

\* In the lower atmosphere, P and T measurements can also contribute to the reconstruction of the atmosphere (Sommer and Boissevain 1967).



## (2) Low-g Accelerometer

This device works on the same general principle as the instrument just discussed. However, it operates during descent, when the acceleration is much less. If turbulence is present, the output signal may be a rather complex function of time, as shown schematically in Figure 20. In a turbulent region, it would not be prudent merely to sample the accelerometer output now and then. Rather, the electronics must include the capability of determining and storing all appropriate integrals of the acceleration. There must be a portion of the entry-descent where both high and low-g accelerometers are operating. This overlap ensures that  $a(t)$  and  $v(t)$  may be continuously integrated throughout entry and descent. During descent, for each "measurement" of the low-g accelerometer, the following quantities are transmitted (at a time  $t_k$ ):

$$v_k = \text{velocity } (t_k)$$

$$h_k = \text{altitude } (t_k)$$

$T_K$  = root-mean-square amplitude of turbulence between  $t_{k-1}$  and  $t_k$

$$= \left[ \frac{1}{t_k - t_{k-1}} \int_{t_{k-1}}^{t_k} (a(t) - \bar{a})^2 dt \right]^{\frac{1}{2}}$$

$\Omega_k$  = average frequency ( $\omega$ ) of turbulence between  $t_{k-1}$  and  $t_k$

$$= \frac{\int_{t_{k-1}}^{t_k} P(\omega) \omega d\omega}{\int_{t_{k-1}}^{t_k} P(\omega) d\omega}$$

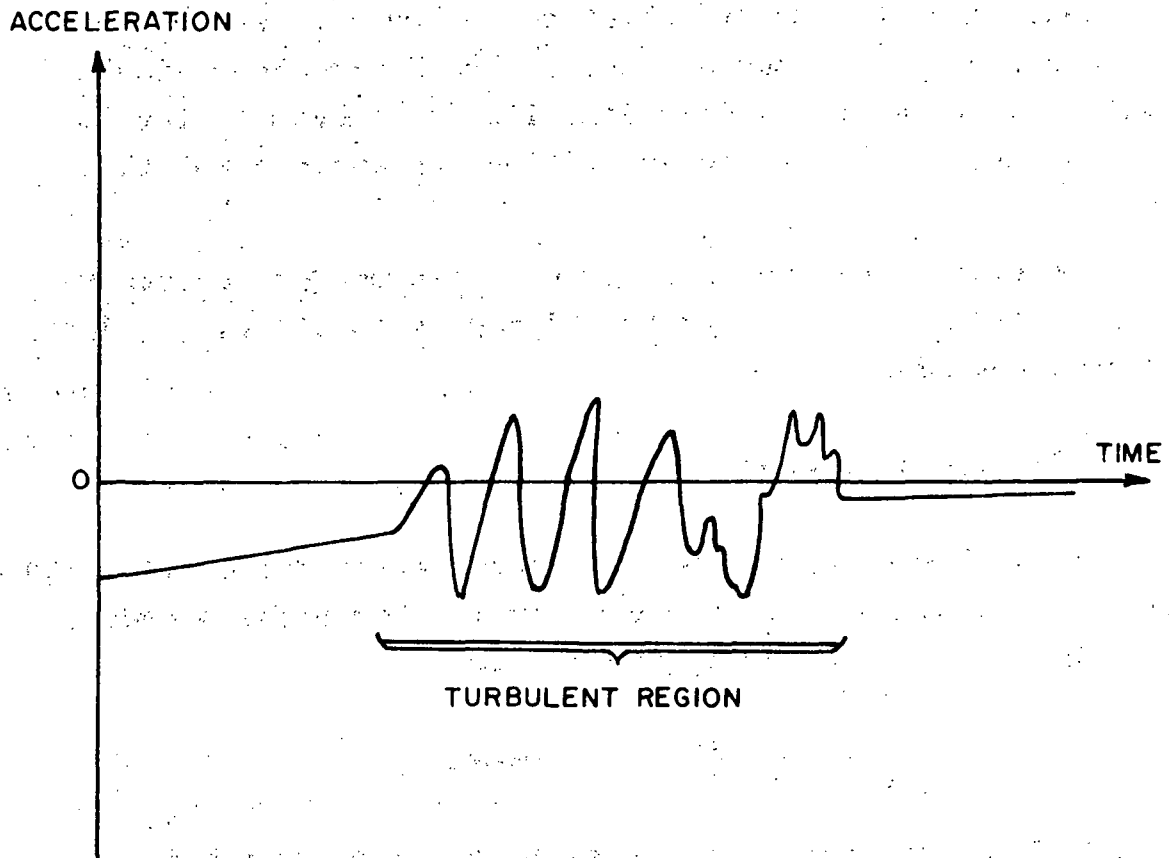


**FIGURE 20. PROBE ACCELERATION VERSUS TIME DURING DESCENT  
(SCHEMATIC)**

The average  $\bar{a}$  is taken between  $t_{k-1}$  and  $t_k$ .  $T_k$  is always greater than zero. It is expected to have some minimum value for a "smooth" atmosphere; greater values indicate turbulence.  $P(\omega)$  is the power spectral density (Fourier transform) of  $a(t)$  between  $t_{k-1}$  and  $t_k$ . 6 bits are allotted for each of the four quantities; thus 24 bits are allotted per measurement of the low-g accelerometer. However, the on-board processor should probably retain several significant figures (decimal) for its continuous estimate of these quantities, to avoid cumulative errors.

Together, the high and low-g accelerometers determine density, altitude, speed, and turbulence as functions of time throughout the mission.

### (3) Pressure Gauge

This should be a simple membrane transducer or capacitance gauge. A correction will be necessary for the probe's speed. The average speed of descent (Uranus) is

$$v_{\text{avg}} = \frac{130 \text{ km}}{30 \text{ min}} = 4.3 \text{ km/min.}$$

This should be compared with the speed of sound, which is

$$v_s = \frac{3 kT}{m} = 48 \text{ km/min}$$

for pure  $H_2$  at  $50^\circ \text{ K}$ . Application of a Bernoulli correction should be straightforward:

$$P_{\text{actual}} = P_{\text{meas}} + \frac{1}{2} \rho v^2 ,$$

since  $\rho$  and  $v$  are known from the low-g accelerometer. A design similar to a pitot tube may be appropriate. Such a device might also measure "air speed" and be compared with the integration - determined velocity measurement and the turbulence measurement, to obtain information regarding local convection.

#### (4) Temperature Gauge

This would probably be a simple Pt-wire thermometer. Again, a correction will probably have to be applied for the fairly high speed of the probe.

#### (5) Nephelometer

This instrument shines a light beam into the atmosphere surrounding the probe and measures the amount of light reflected from it. When the probe is within a cloud, the reflected light is strong; when the probe is in a clear atmosphere, this light is weak. Since clouds are a possibility on Uranus and Neptune, it is important to measure their density (including presence or absence) as a function of atmospheric depth.

### 3.2.3 "Radiative Transfer" Measurements

Besides  $P$ ,  $\rho$ ,  $T$ , and  $\mu$  (composition), another fundamental aspect of a planetary atmosphere is heat transfer (radiative or convective). Some important parameters are:

$$K = \text{opacity (cm}^2 \text{ g}^{-1}\text{)}$$

$$\tau(h_1) = \text{optical depth} = \int_{h_1}^{\infty} K \rho dh \text{ (dimensionless).}$$

A proper theory of heat transfer relates the radiation intensity (solar, and IR emitted from the atmosphere), optical depth, opacity, temperature, and convection (turbulence) throughout the atmosphere. Therefore, to establish a detailed model of heat transfer, it is necessary to measure:

- (a) the attenuated solar flux:

$$I(h) = I_o e^{-\tau(h)}$$

which determines  $\tau(h)$

- (b) IR radiation emitted from the atmosphere (and surface ?), as a function of zenith angle and azimuth
- (c) temperature (previously discussed)
- (d) turbulence (previously discussed)
- (e) opacity; related to composition and clouds (previously discussed).

The optical depth  $\tau$  is related to the extinction cross section  $\sigma$  by

$$\tau(P) = \frac{\sigma P}{\mu g} .$$

Belton, McElroy, and Price (1971) calculate  $\sigma(\lambda)$  under several different assumptions. A typical value is

$$\sigma(5000 \text{ \AA}) = 10^{-27} \text{ cm}^2 \text{ (Rayleigh scattering).}$$

In this case, for Uranus,

$$\tau(P) = (0.3 \text{ bar}^{-1}) \cdot P$$

$\tau = 1$  corresponds to  $P = 3.3$  bars. Calculated values of the optical depth and the attenuation coefficient of sunlight, as a function of pressure, are given in Table 6. These highly simplified calculations imply that most of the sun's energy is absorbed between 1 and 10 bars. Therefore, this is the region where the temperature rises from its previously "constant" value (Trafton 1967). This region is the most important from the point of view of radiative (and perhaps convective) transfer, and it is therefore highly desirable that the entry probe penetrate to at least 10 bars.

#### (1) Visual Spectrophotometer

This instrument measures the attenuated solar flux, from which  $\tau(h)$  may be determined:

$$I(h) = I_0 e^{-\tau(h)}$$

The concept chosen is four channels between  $\sim 0.3 \mu\text{m} - 1 \mu\text{m}$ . The instrument is quite similar to the H:D photometer, since both must sense sunlight. It is felt that a sun-tracking system is too complex. Rather, since the zenith angle (ZA) range of the sun is known, we choose a small sunlight collector of a constant ZA range and  $2\pi$  azimuth (cone-shaped) for these two detectors. A schematic diagram of the sunlight collector is illustrated in Figure 21.  $\theta_{\min}$  and  $\theta_{\max}$  are chosen so that the sun's zenith angle always lines between them during the period of descent. Thus although the probe rotates freely in azimuth, the photometers are continuously receiving sunlight. Though azimuth is not controlled it should be recorded periodically and transmitted to the spacecraft.

Besides sunlight, the visual spectrophotometer can detect any cloud layers the probe passes through.

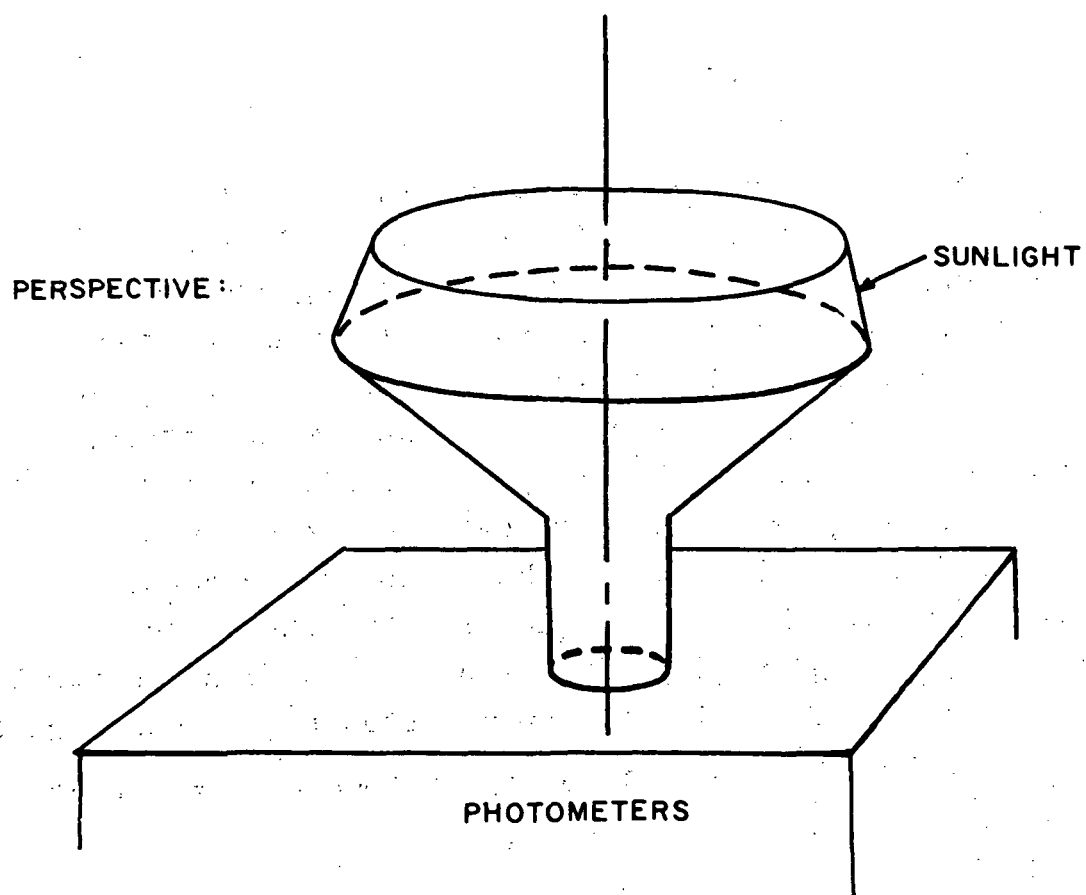
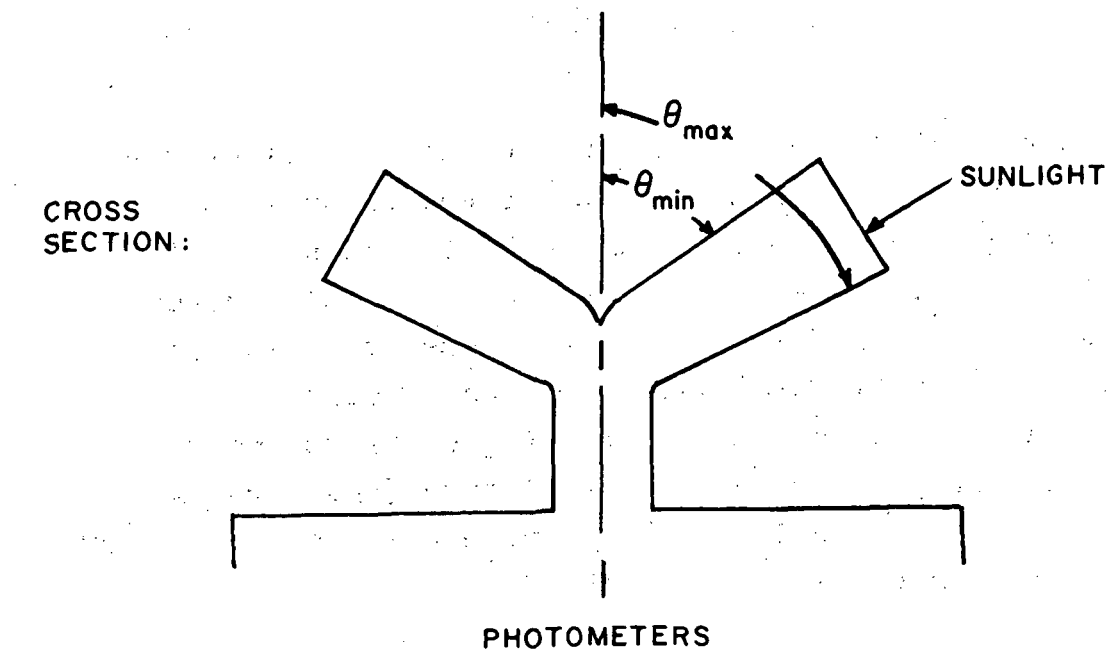


FIGURE 21. SUNLIGHT COLLECTOR (SCHEMATIC)

TABLE 6

OPTICAL DEPTH AND SOLAR RADIATION  
ATTENUATION COEFFICIENT AS FUNCTIONS OF ATMOSPHERIC DEPTH

P(bars)	Optical Depth $\tau$ (5000 Å)	Solar Radiation Intensity <sup>a</sup>
		$\frac{I}{I_o}$ (5000 Å) = $e^{-\tau}$
$10^{-3}$	$3 \times 10^{-4}$	0.9997
$10^{-2}$	$3 \times 10^{-3}$	0.997
$10^{-1}$	$3 \times 10^{-2}$	0.97
1	0.3	0.74
10	3	0.05
100	30	$10^{-13}$

$$^a I_o = 3.8 \text{ watts m}^{-2} \text{ (Uranus)}$$

$$= 1.6 \text{ watts m}^{-2} \text{ (Neptune)}$$



## (2) IR Radiometer

This instrument measures the IR radiation striking the probe. Its data are required to complete the information necessary for a first order understanding of the radiative heat transfer within the atmosphere. The instrument consists of three detectors oriented at zenith angles of  $0^\circ$  (zenith),  $90^\circ$ , and  $180^\circ$  (nadir). The detectors should have as wide a wavelength spread as possible, preferably from  $\lambda \sim 10 \mu\text{m}$  to  $\lambda \sim 80 \mu\text{m}$ . Table 7 gives some of the expected parameters of the IR flux in the atmosphere of Uranus. Column 1 specifies several representative values of pressure during descent from 0.1 to 10 bars. Column 2 gives the corresponding temperature according to the model of Trafton (1967), and column 3 lists the number density of molecules as calculated from the perfect gas law. In column 4 is given the wavelength where the IR emission peaks for the temperature listed, from Wien's displacement law

$$\lambda_{\text{max}} T = \text{constant} = 0.290 \text{ cm} \cdot ^\circ\text{K}.$$

Column 5 lists the IR absorption cross section for this wavelength in pure hydrogen at the appropriate temperature, but with a density of  $10^{20} \text{ cm}^{-3}$ . These cross sections are the sum of the translational and rotational-translational pressure broadened cross sections, and are taken from Belton et al. (1971) (Figures 4 and 5c). Since this is a pressure-broadened cross section, it is proportional to the molecule density, and the cross section corresponding to this density (column 3) is listed in column 6. Finally, in column 7 is given the mean free path  $\ell$  of IR radiation of wavelength  $\lambda_{\text{max}}$  in the atmosphere surrounding the probe:

$$\ell = \frac{1}{n \sigma_{\text{total}}(n)}$$

TABLE 7: INFRARED RADIATION IN THE ATMOSPHERE  
OF URANUS

P(bars)	T(°K)	n(cm <sup>-3</sup> )	$\lambda_{\text{max}}$ ( $\mu\text{m}$ )	$\sigma_{\text{total}}(10^{20}\text{cm}^{-3})$ (cm <sup>2</sup> )	$\sigma_{\text{total}}(n)$ (cm <sup>2</sup> )	$\ell = \frac{1}{n\sigma}$ (km)
0.1	50	$1.45 \times 10^{19}$	58.0	$8 \times 10^{-27}$	$1.2 \times 10^{-27}$	600
0.32	60	$3.87 \times 10^{19}$	48.3	$1.5 \times 10^{-26}$	$6 \times 10^{-27}$	40
1.0	80	$9.05 \times 10^{19}$	36.3	$1 \times 10^{-25}$	$1 \times 10^{-25}$	1
3.2	125	$1.85 \times 10^{20}$	23.2	$2 \times 10^{-25}$	$4 \times 10^{-25}$	0.1
10	150(?)	$4.85 \times 10^{20}$	19.3	$4 \times 10^{-25}$	$2 \times 10^{-24}$	0.01

To a first approximation, this represents the distance from which the observed IR flux is originating. For example, let us consider the "sideways-looking" IR detector ( $ZA = 90^\circ$ ). This detector "sees" a horizontal column of atmosphere, all points of which are at the same pressure and presumably have the same values of  $T$ ,  $n$ ,  $\lambda_{\max}$ , and  $\ell$ . In this case the value of  $\ell$ , determined from measurements of  $P$  and  $T$  on the probe, also represents approximately the maximum distance from which IR radiation is received by the probe, i.e. the depth to which the probe "sees". For the "up" and "down" looking detectors, this is true only if  $\ell$  is much less than a scale height or any other distance over which temperature or composition changes significantly. Thus, it would probably be true at  $P = 10$  bars, untrue at  $P = 0.1$  bars.

Each IR detector measures the total flux incident upon it. One important immediate result is the radiative heat flux, determined by comparing the outputs of the "up" and "down" detectors. These should be correlated with the measurements of temperature and turbulence to determine whether or not the planet has any internal heat generation. A search for variation of the flux with azimuth ( $ZA = 90^\circ$ ) could provide information regarding clouds or other atmospheric structure, particularly at the higher altitudes. More generally, the results of the IR radiometer are needed to complete the measurements of all major variables in the heat transfer theory: solar flux, opacity, IR flux, composition, temperature, and convection (turbulence). Together this set of variables provides the redundancy necessary to obtain a fairly accurate and self-consistent theory of atmospheric structure and activity.

Unfortunately, it does not appear that the "down" - looking detector can provide significant information regarding the deep atmosphere below. At  $P = 10$  bars, for any reasonable temperature, the depth to which the probe "sees" is less than 1 kilometer, and therefore much less than a scale height.

### 3.2.4 Summary of Scientific Payload

Table 8 lists the scientific payload which has just been derived. For each instrument the estimated mass, power, size, and bits per measurement is listed. Unless otherwise indicated, these numbers were taken from the AVCO study of Jupiter atmospheric entry (1971a). The estimates of the total mass, power, and volume of the scientific payload are  $\sim 11$  kg,  $\sim 17$  watts, and  $\sim 7,000 \text{ cm}^3$  respectively. In summary, the entry probe will measure atmospheric composition, density, pressure, temperature, turbulence amplitude and frequency, cloud density, solar radiation intensity and optical depth, and emitted IR radiation, as functions of altitude, from pressures of  $\sim 0.1$  bars to 10 bars. It will not measure the composition of the ionosphere or upper atmosphere; also, it will not search for specific constituents (except  $\text{CH}_3\text{D}$ ), life, atmospheric electricity, thunder, magnetic field anomalies, etc. We feel that the chosen payload is appropriate for a first-generation exploratory probe to Uranus and Neptune. Later probes can go deeper and carry more sophisticated instruments, based on the information returned by this first probe mission.

TABLE 8  
ENTRY PROBE SCIENTIFIC PAYLOAD  
(Ref. for numbers - AVCO (1971a) unless otherwise indicated)

Instrument	Mass (kg)	Power (w)	Volume (cm <sup>3</sup> )	Bits per meas.
<u>Composition:</u>				
Mass Spectrometer	4.5 <sup>a</sup>	12	5650	330 <sup>c</sup>
H-D Photometer	0.5 <sup>b</sup>	0.2	100	9 <sup>i</sup>
<u>Equation of State:</u>				
High-g accelerometer	0.5	1	100	(28 <sup>h</sup> )
Low-g accelerometer	0.9	2	160	18
Pressure Gauge	0.9	0.1	160	9
Temperature gauge	0.5	0.2	250	12
Nephelometer	2.0	3	1600	9
<u>Radiative Transfer:</u>				
Visual Spectrophotometer	2.3 <sup>e,f</sup>	0.4	500	40
IR Radiometer	0.5	1.5	410	30 <sup>g</sup>
TOTAL	12.6	20.4	8930	

<sup>a</sup> Avg. AVCO and H. Niemann (private communication)

<sup>b</sup> AVCO = 0.35 lbs.  $\approx$  0.15 kg.

<sup>c</sup> (15<sup>d</sup> bits/sig. mass) x (22<sup>e</sup> sig. masses). Mass range = 1-40 amu.

<sup>d</sup> PAET (Ames 1971b)

<sup>e</sup> Author's estimate

<sup>f</sup> Includes fiber-optics light collector from all zenith angles. Based on AVCO "aerosol photometer", 1  $\mu$ m, 0.65 lbs.  $\approx$  0.3 kg.

<sup>g</sup> 3detectors x 10 bits/detector (AVCO)

<sup>h</sup> Not counted in total, because measures during entry, not descent (4 accelerometers, each 7 bits; AVCO)

<sup>i</sup> AVCO's value = 10.

## 4. PROBE DESIGN

### 4.1 Data Transmission

Whenever one of the scientific instruments makes a measurement, it gathers a certain amount of information. A given number of bits must be allotted for transmitting this information to the spacecraft, and thence to Earth. Bit allotments for the various instruments are given in Table 9, from which it may be seen that the mass spectrometer requires a large number of bits per measurement (330), whereas the other instruments each require much smaller numbers (10 to 30 apiece).

It was decided to include on the probe the capability of storing all data from the entire mission. First, during entry, the data from the high-g accelerometer are gathered and stored; 7000 bits are allowed for this (see Table 9). Then, during descent, data are gathered by the other instruments, and stored. The entire storage is scanned and transmitted several times during the descent. This redundancy of transmission insures greater reliability.

In answer to the question, "when should each instrument make a measurement?", we limited ourselves to a fairly simple approach. Each instrument, except the mass spectrometer, is assumed to make the same number of measurements. The number 90 was chosen, since it satisfies both scientific and data-handling requirements. Because the mass spectrometer accumulates so many bits per measurement, the data transmission system could not accept as many as 90 measurements from it. Instead, one-third as many (30) measurements were assumed. One simple scheduling procedure would be to allow a constant interval of time ( $\Delta t$ ) between measurements, for each instrument. In this case, because the probe is traveling much more slowly near the end of descent, the lower altitudes would be studied more thoroughly than the

TABLE 9: DATA PARAMETERS FOR EACH INSTRUMENT<sup>a</sup>

INSTRUMENT	DATA PER MEASUREMENT		ALLOTMENT OF DATA (BITS)	INDEPENDENT VARIABLE OF MEASUREMENT	
Mass Spectrometer	330	(~22 significant masses) x (15 bits/mass)		Altitude ( $\Delta h$ )	
H:D Photometer	9	3 OD		Altitude ( $\Delta h$ )	
High-g Accelerometer <sup>b</sup>	28	4 <sup>c</sup> detectors, each 2 OD plus a sign		Time ( $\Delta t$ )	
Low-g Accelerometer	24	4 quantities: v, h, turbulence amplitude, turbulence frequency, each 2 OD		Time ( $\Delta t$ )	
Pressure Gauge	9	3 OD		Altitude ( $\Delta h$ )	
Temperature Gauge	12	4 OD		Time ( $\Delta t$ )	
Nephelometer	9	3 OD		Altitude ( $\Delta h$ )	
Visual Spectrophotometer	40	4 channels, each 2 OD plus 1 OD exponent, plus 4 bits for azimuth recorder		Time ( $\Delta t$ )	
IR Radiometer	30	3 detectors, each 2 OD + 4 bit exponent		Time ( $\Delta t$ )	

<sup>a</sup> "OD" = octal digit = 3 bits

<sup>b</sup> The high-g accelerometer collects a total of (28 bits/meas.) x (2 meas./sec.) x (~120 sec. of entry)

<sup>c</sup> One 3-axis and one single-axis instrument (AVCO 1971).

upper ones (more measurements per kilometer). Another procedure would be to allow a constant interval of altitude ( $\Delta h$ ) between measurements. In this case, data would pour in more rapidly at the beginning of descent than at the end. The procedure chosen was a combination of these. An individual instrument operates according to either the  $\Delta t$  or  $\Delta h$  procedure, whichever is more appropriate. Where we expect equally interesting information from all altitudes, measurements are made at constant  $\Delta h$ ; this is true of measurements by the mass spectrometer, H:D detector, nephelometer, and pressure gauge. On the other hand, where we expect more interesting information toward the end of descent (1 to 10 bars), measurements are made at constant  $\Delta t$ ; this is true of all the other instruments. These measurement modes are summarized in the last column of Table 9.

The high-g accelerometer accumulates  $\sim 7000$  bits of data during the high-speed entry portion of the mission. These data are stored, then transmitted after the aeroshell is dropped. The total accumulated data for the science instruments is approximately 28,000 bits for both Uranus and Neptune, as shown in Figure 22. (The descent parameters, although very different for the two planets, nevertheless have been chosen so as to make the two data-vs.-time curves virtually identical; thus only one Figure is needed). A nominal scan rate of 50 bits/sec was chosen for data transmission, resulting in about 4 scans through the entire stored data. Data transmission reliability can be further strengthened by interleaving current data with stored data in case of probe failure. For example, the first mass spectrometer measurement might be transmitted along with some of the stored high-g accelerometer data as the first scan begins. Also, the fourth scan could omit the data from the high-g accelerometer, since the latter data will have been scanned three times previously.



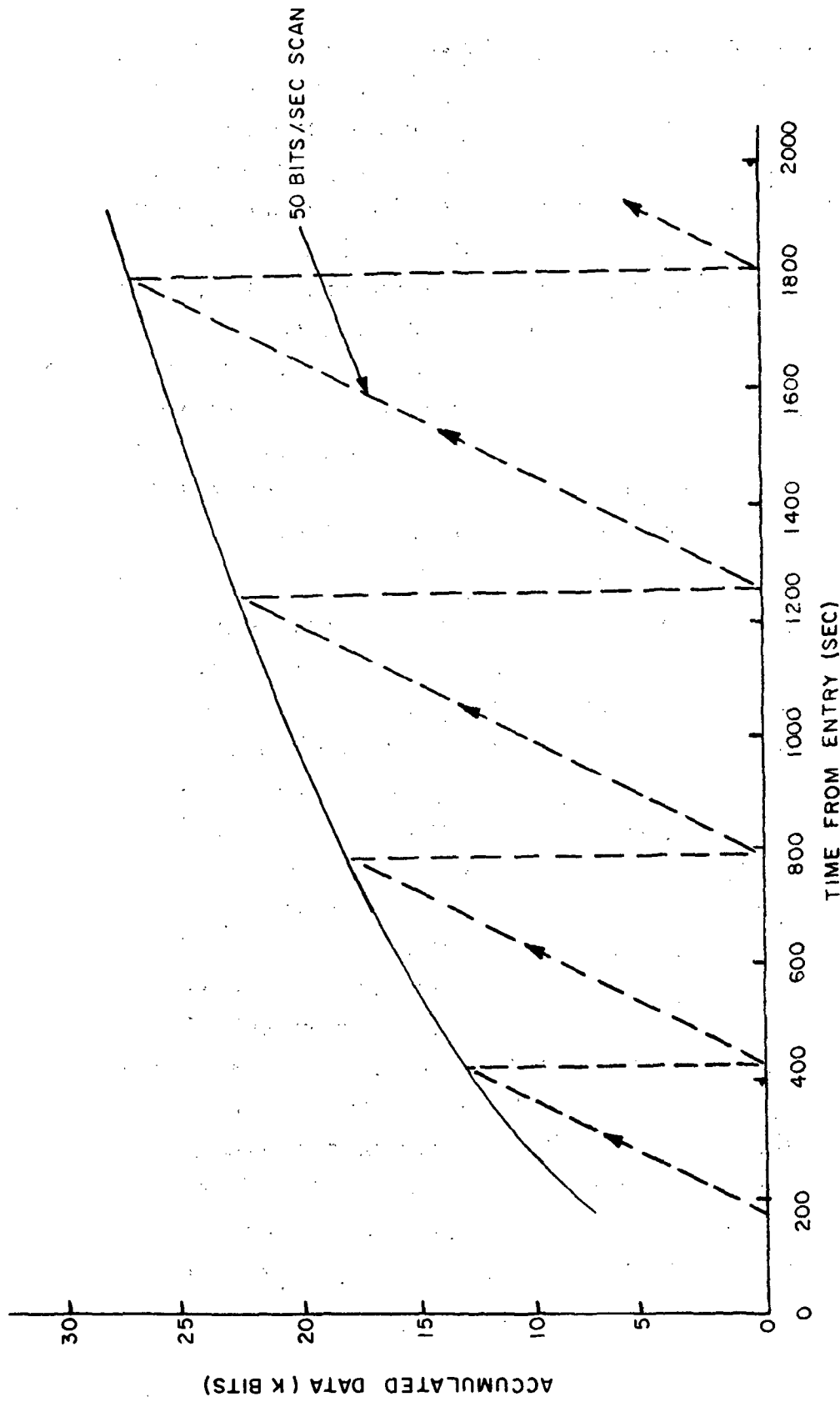


FIGURE 22. DATA ACCUMULATION AND TRANSMISSION DURING DESCENT (URANUS AND NEPTUNE)

About 200 seconds after entry, roughly 7000 bits have been received and stored from the high-g accelerometer. As descent begins and continues, the total amount of stored data increases from 7000 bits (solid line). The stored data are scanned and transmitted several times during descent. The dashed line illustrates which portion of the data is being transmitted at a given time. Its slope corresponds to a transmission rate of 50 bps.

Given the amount of data, communication distance, and nominal data rate (50 bits/sec), the probe transmitter power requirements can be determined for the four mission cases. Frequency shift keying (FSK) was selected for data modulation, since atmospheric turbulence has little effect upon the FSK signal compared to phase shift keying (PSK). Data transmission occurs between the probe transmitting antenna (3 db, 90° zenith angle) to the spacecraft omni antenna, at a frequency of 1 GHz. The required transmission power  $P$  is given by

$$P = \frac{(4\pi)^2 R^2 kT \rho C}{G_T G_R \lambda^2}$$

Definitions and estimates of these quantities are as follows:

- $R$  = communication distance (20,000 km to 345,000 km; see Table 3)
- $k$  = Boltzmann's constant =  $1.38 \times 10^{-23}$  joule  $^{\circ}\text{K}^{-1}$
- $T$  = receiver noise temperature =  $300^{\circ}\text{K}$
- $\rho$  = signal-to-noise ratio = 12.6 (11 db)\*
- $C$  = data transmission rate = 50 bits per second
- $G_T$  = gain of transmitting antenna = 2  
(3 db; 90° zenith angle)
- $G_R$  = gain of receiving antenna = 1  
(0 db; omni antenna)
- $\lambda$  = wavelength = 30 cm

Using this expression, we find the required transmission power to be ~270 watts for Uranus/1981 SUN mission, and ~ 1 to 15 watts for the other missions. Attenuation losses were assumed to be negligible, based on the expected composition of the atmospheres and the low spacecraft zenith angle (see De Wolf et al. 1971).

\* Assuming a bit error probability =  $P_e = 10^{-3}$ . Ames (1971a) includes a curve relating  $P_e$  and  $\rho$  for frequency shift keying.

## 4.2 Description of Subsystems

Based on the scientific payload previously discussed (Section 3) and the subsystems described by Martin-Marietta (1971) for a Jupiter atmospheric entry probe, we have derived an estimate of the subsystems required for a Uranus-Neptune entry probe, and the mass and power of each. This list is given in Table 10. Because the probe descends only to 10 bars, no pressure vessel is included.

We wish to establish the total power requirement for operating all probe subsystems except descent thermal control. As explained in Section 4.1, the output power of the probe transmitting antenna need be at most  $\sim 15$  watts for each mission except Uranus/SUN 1981, for which it must be  $\sim 270$  watts. Assuming a transmitter efficiency of 33%, the total power required for data transmission is  $\sim 45$  watts (or 810 watts). Since acquisition, entry, and descent last about 1 hour, the corresponding stored energy must be  $\sim 45$  watt-hours (or 810 w-h). The remaining subsystems consume about 30 watts, or about 30 w-h of energy. Furthermore, during the deployment phase, about 150 w-h are required for tracking and temperature stabilization. Therefore, the total stored energy required is  $\sim 225$  w-h (or  $\sim 990$  w-h).

Next, we consider descent thermal control. Probe thermal insulation was assumed to be a combination of styrofoam ( $K = 0.86 \times 10^{-4} \text{ cal cm}^{-2} \text{ s}^{-1} (\text{°K/cm})^{-1}$ ) and superinsulation ( $\epsilon \cong 3 \times 10^{-4}$ ). Approximate calculations indicated that the descent heat loss should be about 280 watts. First, we assume that all of this is produced by the transmitter and other subsystems (i.e. there is no additional heater). Therefore, the transmitter must release  $280 \text{ w} - 30 \text{ w} = 250$  watts of heat. Since its efficiency is 33% it broadcasts 125 watts, and consumes 375 watts total. This transmitter is sufficient for all mission cases except Uranus/SUN 1981, and accordingly is adopted for these three cases. Thus, the total energy consumed during descent

TABLE 10: ENTRY PROBE SUBSYSTEMS

<u>SUBSYSTEM</u>	<u>MASS (KG)</u>	<u>POWER (w)</u> (during Descent)
Science	12.6	20
Data Handling & Communications	9.5	375
Power and Power Conditioning	12.0	5
Cabling	5.0	-
Mechanisms & Pyrotechnics	8.0	5
Structures & Heat Shield	32.0	-
Insulation	12.0	-
Attitude Control	10.0	-
Propulsion	10.0	-
Subtotal	111.1	-
Contingency (15%)	16.7	-
TOTAL	127.8	405

is  $\sim 405$  w-h, and the total energy consumed during the mission is 555 w-h. A battery performance assumption of 90 w-h/kg leads to a battery mass of  $\sim 6$  kg. Including battery contingency, a total of 12 kg was allowed for power and power conditioning systems. (By the same line of reasoning, the total stored energy required for the Uranus/SUN 1981 mission is  $\sim 990$  w-h, corresponding to a battery mass of  $\sim 11$  kg. This mission would involve a power system which is expanded over the nominal one).

The total post-entry mass of the probe is 128 kg which includes a 15% growth factor as contingency. The heat shield mass allowance was taken as 14% of the entry mass, or in this case 16 kg (see Section 2.2). The total mass addition to the spacecraft is estimated to be about 170 kg, including the estimated mass due to spacecraft modifications.

The overall size of the probe is determined from the ballistic coefficient, using the relation

$$A = \frac{M}{BC_D} = \pi \left(\frac{D}{2}\right)^2$$

where

- A = aeroshell area
- M = probe mass
- B = ballistic coefficient
- $C_D$  = drag coefficient
- D = aeroshell diameter

The probe mass estimate has been given in Table 10 and a ballistic coefficient of  $150 \text{ kg/m}^2$  was chosen in Section 2. A  $120^\circ$  aeroshell is assumed for which the drag coefficient is

$$\begin{aligned} C_D &\cong 1.6 \text{ (supersonic; entry) (Campbell 1967)} \\ &\cong 0.6 \text{ (subsonic; descent) (Owens 1965).} \end{aligned}$$

Table 11 then gives the computed probe sizes for the different cases of interest. The effective probe diameter must be  $\sim 0.8$  meters for entry on either planet, and  $\sim 1.0$  m for descent on Uranus. It must be  $\sim 1.8$  meters for a free-fall descent on Neptune. In order to maintain a fixed probe size (for commonality) for Uranus and Neptune, a small parachute would have to be provided for Neptune descents.

At  $t = -15$  days, when the probe is released from the parent spacecraft, the deflection system performs the maneuver that puts the probe on the proper trajectory for entry. Tracking is performed for about an hour to ensure that the trajectory is correct. As entry begins, the deflection and attitude control subsystems are jettisoned. At the end of entry, the parachute is deployed, and the heat shield is jettisoned. Remaining is a "descent aeroshell" which has the same general shape and ballistic coefficient as the heat shield, but contains some windows for scientific instruments. After the heat shield is jettisoned the parachute is released for Uranus missions but retained for Neptune missions in order to maintain the correct descent ballistic coefficients.

TABLE 11: PROBE SIZES AND BALLISTIC COEFFICIENTS

ENTRY PHASES	PROBE PARAMETERS				
	M	B	$C_D$	A	D
Entry	128 kg	150 kg/m <sup>2</sup>	1.6	.53 m <sup>2</sup>	.82 m
Descent (Uranus)	86	200	0.6	.72	.96
Descent (Neptune)	86	55	0.6	2.60	1.82

## 5. COMPARISON OF RESULTS WITH PREVIOUS STUDIES

In this study we have examined the value and feasibility of entry probes into the atmospheres of Uranus and Neptune. A comparison of our results with those of previous studies of Jupiter atmospheric entry is presented in Table 12. As can be seen from that table, probes which descend to depths beyond 10 bars are generally much heavier than those which do not, because of the necessity of a pressure vessel to protect the instruments. The IITRI and Ames probes are small and simple, and do not descend beyond 10 bars. On the other hand, the Avco and Martin-Marietta probes are heavier and more complex, and descend to several hundred bars pressure. The IITRI and Ames probes are quite similar. IITRI includes every instrument that Ames included, plus an H:D photometer (to resolve ambiguities in the mass spectrometer results), a visual spectrophotometer (to measure optical depth, and provide all parameters necessary for a model of radiative transfer), and a nephelometer.

Some instruments which are included on other probes, which we decided were not worth their weight and power penalty, are summarized in Table 13, along with our reasons for not including them. Particularly where relative scientific values are concerned, such reasoning must inevitably be somewhat subjective, but we nevertheless feel that the choices are reasonable.

It has been suggested that there be as much commonality as possible between probes to Jupiter-Saturn and probes to Uranus-Neptune, to minimize the necessity for new hardware. With respect to scientific instruments, this suggestion appears valid. Every instrument suggested here would also be very useful on an entry probe to Jupiter or Saturn. With respect to



TABLE 12  
COMPARISON OF RESULTS OF THIS STUDY (URANUS-NEPTUNE) WITH THOSE BY AVCO, AMES, AND MARTIN-MARIETTA (JUPITER)

IITRI ASTRO SCIENCES		AVCO	AMES	MARTIN-MARIETTA
Target Planet(s)	Uranus- Neptune	Jupiter	Jupiter	Jupiter
Atmosphere Depth (Bars)	10	3.5 - 525	10	20 - 300***
Spacecraft	Unspecified	TOPS and Pioneer	Pioneer	TOPS and Pioneer
Pressure Vessel Considered	No*	Yes	No	Yes
Entry Angle(s) (Deg.)	27 - 50	21 - 33	23	10
Entry Velocity (km/sec)	25 - 30	49	50	59.6
Max. Deceleration (Earth G/s)	380 - 580	260 - 1250	1000	393 - 718
Communications	Through S/C	Through S/C & Direct to DSN	Through S/C	Through S/C and Direct to DSN
Entry & Descent Duration (Hrs.)	0.5	0.4 - 1.0	0.5	0.5 - 3.0
Total Probe Mass (kg)	128	278 - 387	88	300 - 580
Science Payload	Baseline	Small Nominal** Expanded	Baseline	Small Nominal Expanded
Depth (Atm.)	10	3.5 - 525	10	20
Instrument Mass (kg)	12.6	7.3	16.0	4.5
INSTRUMENTS				
Eq. of State:				
Pressure	Pressure	Pressure	Pressure	Pressure
Temperature	Temperature	Temperature	Temperature	Temperature
High-g Accel.	High-g Accel.	High-g Accel.	High-g Accel.	High-g Accel.
Low-g Accel.	Low-g Accel.	Low-g Accel.	Low-g Accel.	Low-g Accel.
Composition:				
Mass Spec.	Gas Chrom/ Mass Spec. Ion Mass Spec.	Gas Chrom/ Mass Spec. Ion Mass Spec. H:D Phot.	Mass Spec.	Gas Chrom/ Mass Spec.
H:D Phot.		Methane Abun. Ammonia Abun.		H:D Phot.
Nephelometer		Cloud Det. Aerosol Part.		Nephelometer
Radiative Transfer:		UV Spec. Cloud Det. Aerosol Part. Evaporimeter		Nephelometer
Visual Spectro- photometer				Visual Photometer
IR Radiometer		IR Radiometer	IR Radiometer	IR Radiometer
Other:		Lightning Magnetometer RF Click		Lightning

\* Considered in Interim Design to 100 bars

\*\* Dayside Mission

\*\*\* Split Probes Considered to 1000 bars

TABLE 13: INSTRUMENTS NOT INCLUDED IN SCIENTIFIC PAYLOAD

Instrument(s)	Reason For Omitting
Gas Chromatograph	Complex; can make only 1 measurement/5 minutes
Ion Mass Spectrometer	Measures ionospheric composition during entry; given the composition of the lower atmosphere, the former is not of prime scientific importance  Requires window in heat shield, therefore lessens simplicity and reliability
Photometers and UV Spectrometer to measure CH <sub>4</sub> , NH <sub>3</sub> , H <sub>2</sub> S abundances, and to search for life	Space on the probe did not permit further composition - measuring instruments.  Life should probably not be sought on Uranus/Neptune unless it is found on Jupiter, particularly not on a first mission
Lightning Detectors (Optical and RF Click)	Less important than nephelometer.
Magnetometer	Data from probe would be relatively unimportant compared to data from parent spacecraft (presumed to carry a magnetometer)*. Also, a boom would be necessary, which may be incompatible with a small, first-generation entry probe design.

\* This is perhaps not true for the Uranus/1979 JUN mission, with the high periapse radius, (12.8 planetary radii).

the engineering design of the probe and its subsystems, the feasibility of complete commonality is not so clear, because of the very different entry velocities and relative mass ablation losses expected at the different planets.

## 6. CONCLUSIONS

Our overall conclusion is that in-situ scientific study of the atmospheres of Uranus and Neptune would be feasible. The most important measurement is that of atmospheric composition, which could significantly contribute to our knowledge of the origin of the solar system, and perhaps even of the universe. Studies of planetary atmospheric dynamics would also be extremely interesting. We further conclude that an entry probe could be carried on a Grand Tour mission with minimal impact upon the spacecraft, and that a first-generation probe should be designed to penetrate to an atmospheric depth of about 10 bars. Preliminary estimates of overall mass, power, and size of such a probe are  $\sim 130$  kg,  $\sim 400$  watts, and  $\sim 0.4 \text{ m}^3$ , respectively. The descent trajectory may be chosen so that the probe descends to 10 bars in 30 minutes, as required by line-of-sight constraints on transmission time.

This has been only a preliminary study, and much further work is necessary, of which specific examples have been noted several times throughout the report. With respect to trajectory dynamics, some necessary investigations for the future are entry profiles with different He/H ratios, entry and descent profiles in non-isothermal atmospheres (variable scale height), and more detailed analysis of guidance and communications. Relative to the scientific payload, some necessary projects are detailed error analysis of altitude determination by integration of accelerometer output, detailed analysis of possible ambiguities in mass spectrometer output and their elimination, and analysis of the accuracy required of the radiative transfer measurements to provide meaningful inputs to new theories of the thermal state of the atmospheres. More detailed design of probe subsystems is also desirable, with particular emphasis on the data encoding, transmission rate, and transmission power required as a function of time for different entry points, so as to try to discover possible entry points where data transmission time (and thus attainable depth) may be maximized for a given descent rate. Furthermore, more specific design of all subsystems is desirable, especially with respect

to thermal control. The impact of the probes on the parent spacecraft should be studied in more detail. Finally, direct entry missions (not involving a parent flyby) should be considered. In short, more detailed analysis of all phases of these missions is desirable. However, we believe that this preliminary study has shown that Uranus-Neptune entry probes are valuable and basically feasible.

## REFERENCES

- Allen, C. W. 1963, Astrophysical Quantities, London, The Athlone Press.
- Ames 1971a, "Jupiter Atmospheric Entry Probe Study," Oral Presentation to Science Advisory Group, October 21.
- Ames 1971b, "PAET: Planetary Atmosphere Experiments Test," September.
- AVCO 1971, "A Study of a Jupiter Atmospheric Entry Probe Mission," Report AVSD-0372-71-RR, Wilmington, Mass., AVCO Systems Division.
- Beer, R., Farmer, C. B., Norton, R. H., Martonchik, J. V., and Barnes, T. G. 1972, "Jupiter: Observation of Deuterated Methane in the Atmosphere," Science, 175, 1360.
- Belton, M. J. S., McElroy, M. B., and Price, M. J. 1971, "The Atmosphere of Uranus," Ap. J., 164, 191.
- Campbell, J. F. 1967, "Longitudinal Aerodynamic Characteristics of Several High-Drag Bodies at Mach Numbers from 1.50 to 4.63," NASA TN D-3915.
- Cameron, A. G. W., 1972, "Elemental and Isotopic abundances of the Volatile Elements in the Outer Planets," to be published.
- Dawson, P. H., Hedman, J. W., and Whetten, N. R. 1969, "A Simple Mass Spectrometer," Rev. Sci. Instr., 40, 1444.
- DeWolf, D. A. et al. 1971, "Investigation of Line-Of-Sight Propagation in Dense Atmosphere, Phase 3, Part 1," NASA STAR No. N72-19427.
- Divita, E. L., et al. 1970, "TOPS Spacecraft and the Missions," Astronautics and Aeronautics, AIAA, New York, September.
- Freeman, K. C. and Lynga, G. 1970, "Data for Neptune from Occultation Observations," Ap. J., 160, 767.
- Herzberg, G. 1945, Molecular Spectra and Molecular Structure, II. Infrared and Raman Spectra of Polyatomic Molecules, New York, Van Nostrand.
- Herzberg, G. 1950, Molecular Spectra and Molecular Structure, I. Spectra of Diatomic Molecules, New York, Van Nostrand.
- Hunten, D. M. 1971, "Composition and Structure of Planetary Atmospheres," Space Science Reviews, 12, 539-599. Also printed in Physics of the Solar System, NASA TM X-65702, STAR No. N71-37406.

## REFERENCES - Continued

- Kovalevsky, J. and Link, F. 1969, "Diameter, Oblateness, and Optical Properties of the Upper Atmosphere of Neptune from the Occultation of the STAR BD-17°4388," *Astron. and Astrophys.*, 2, 398 (in French).
- Kuzmin, A. D., and Losovskii, B. Y. 1971, "Measurements of the Radio Emission of Uranus at 8.22 mm and Some Properties of the Planet's Atmosphere," *Solar System Research*, 5, #1, p.18.
- Martin-Marietta 1971, "Jupiter Atmospheric Entry Mission Study," Contract JPL 952811; S. J. Ducsay, Study Manager; Denver, Colorado.
- Munch, G. and Neugebauer, G. 1971, "Jupiter: An Unidentified Feature in the 5-Micron Spectrum of the North Equatorial Belt," *Science*, 174, 940.
- Newburn, R. L., Jr. and Gulkis, S. 1971, "A Brief Survey of the Outer Planets and Their Satellites," JPL Technical Report No. 32-1529, NASA CR 118-180, STAR No. N71-24355.
- Nier, A. O. and Hayden, J. L. 1971, "A Miniature Mattauch-Herzog Mass Spectrometer for the Investigation of Planetary Atmospheres," *Int. J. Mass Spectrom. Ion Phys.*, 6, 339.
- Owen, T. 1967, "Comparisons of Laboratory and Planetary Spectra IV. The Identification of the 7500 Å Bands in the Spectra of Uranus and Neptune," *Icarus*, 6, 108.
- Owens, R. V. 1965, "Aerodynamic Characteristics of Spherically Blunted Cones at Mach Numbers from 0.5 to 5.0," NASA TN D-3088.
- Price, M. J. and Waters, J. I. 1971, "Preliminary Analysis of Uranus/Neptune Entry Probes for Grand Tour Missions," (Interim Study Report), Astro Sciences/IITRI Report No. M-27.
- Prinn, R. G., and Lewis, J. S. 1972, "Uranus Atmosphere: Structure and Composition," submitted to *Ap. J.*
- Seiff, A. 1968, "Direct Measurements of Planetary Atmospheres by Entry Probes," AAS Paper 68-187.
- Sommer, S. C., and Boissevain, A. G. 1967, "Atmosphere Definition with a Free-Falling Probe," *Astro. and Aero.*, Feb., 1967, p. 50. See also NASA STAR No. N67-23302, a more technical version of the same results.
- Swenson, B. L., Edsinger, L. E., Manning, L. A., Norman, S. M., Sinclair, K. F., Stratton, A. J. and Tindle, E. L. 1971, "Preliminary Analysis of an Atmosphere -Entry Probe Mission to Jupiter," NASA TM X-2338.
- Suess, H. E. and Urey, J. C. 1956, "The Abundances of the Elements," *Revs. Mod. Phys.*, 28, 53.

IIT RESEARCH INSTITUTE

REFERENCES - Continued

- Tauber, M. E. 1970, Ames Research Center, Moffett Field, California (Private Communication).
- Tauber, M. E. 1971, "Heat Protection for Atmospheric Entry into Saturn Uranus, and Neptune," 17th Annual Meeting, American Astronautical Society, Preprint No. AAS-71-145.
- Teifel, V. G., and Kharitonova, G. A. 1970, "The Molecular Rotational Temperature of Uranus and an Upper Limit on the Pressure in its Outer Atmosphere," Soviet Astronomy, A. J., 13, No. 5, pp. 865-873.
- Trafton, L. M. 1967, "Model Atmospheres of the Major Planets," Ap. J., 147, 765.
- Winkler, H. et al. 1971, "A Study of Jupiter Atmospheric Probe Missions," Final Oral Presentation to JPL, AVCO Corporation.



## DISTRIBUTION LIST

NASA Headquarters  
Washington, D. C.

Mr. J. Moore, Code SL (12 copies)  
Mr. S. Grivas, Code AAD-4  
Dr. George Jacobs, Code SB  
Mr. B. C. Lam, Code SV  
Mr. R. L. Lohman, Code MTY  
Mr. J. B. Mahon, Code SV  
Mr. J. Mitchell, Code SG  
Dr. M. Mitz, Code SL  
Dr. M. Molloy, Code SPR  
Dr. J. W. Wild, Code MTE

NASA-Ames Research Center  
Moffett Field, California

Dr. Fred Casal, MAD  
Mr. William Johnson, Library Branch  
Mr. Howard Matthews, Manager, Advanced Pioneer Studies  
Dr. Paul Swan, Assistant Director, MAD

NASA-Goddard Space Flight Center  
Greenbelt, Maryland

Mr. George Levin  
Dr. Rudolf Stampfl  
Dr. F. D. Vonbun, Director, Mission Analysis Office  
Mr. John M. Weaver, Library Branch

University of Arizona  
Lunar and Planetary Laboratory  
Tucson, Arizona

Dr. Gerard Kuiper

Jet Propulsion Laboratory  
4800 Oak Grove Drive  
Pasadena, California

Dr. R. Bourke  
Mr. J. Long, 180-303  
Dr. R. Mackin, 186-133  
Dr. Donald G. Rea

NASA-Lewis Research Center  
21000 Brookpark Road  
Cleveland, Ohio 44135

Mr. Robert J. Lubick  
Mr. G. Mandel, Library Branch

IIT RESEARCH INSTITUTE

DISTRIBUTION LIST - Continued

NASA-Manned Spacecraft Center  
Houston, Texas

Mr. J. M. Eggleston  
Mr. Charles M. Grant, Jr.  
Mr. A. Sanders, Library

NASA-Marshall Space Flight Center  
Huntsville, Alabama 35812

Mr. H. J. Dudley  
Mr. C. Guttman  
Dr. D. Hale  
Mr. R. Harris  
Mr. John L. Tidd

Office of Science and Technology  
Executive Office Building  
Room 282  
Washington, D. C.

Mr. Gordon Moe

Battelle Memorial Institute  
505 King Avenue  
Columbus, Ohio 43201

Mr. Bruce W. Davis, Director, NASA Launch Vehicle Planning  
Project

Mr. Donald S. Edgecombe

NASA-Langley Research Center  
Hampton, Virginia

Library

NASA Scientific and Technical  
Information Facility  
Post Office Box 33  
College Park, Maryland 20740

(3 copies, including 1 reproducible copy)